WAVELET TRANSFORM BASED ALGORITHMS FOR LOAD COMPENSATION USING DSTATCOM

A Project Report

submitted by

MUS-AB.A

in partial fulfilment of the requirements
for the award of the degree of

Master of Technology (Power Systems and Power Electronics)
and Bachelor of Technology
in
Electrical Engineering

DEPARTMENT OF ELECTRICAL ENGINEERING
INDIAN INSTITUTE OF TECHNOLOGY MADRAS.

MAY 2015

By the Grace of Almighty Allah

THESIS CERTIFICATE

This is to certify that the thesis titled **WAVELET TRANSFORM BASED ALGORITHMS FOR LOAD COMPENSATION USING DSTATCOM**, submitted by **MUS-AB.A**, to the Indian Institute of Technology, Madras, for the award of the degrees of **"BACHELOR OF TECHNOLOGY"** and **"MASTER OF TECHNOLOGY"**, is a bonafide record of the project work done by him under my supervision. The contents of this thesis, in full or in parts, have not been submitted to any other Institute or University for the award of any degree or diploma.

Dr. Mahesh Kumar
Professor
Dept. of Electrical Engineering
IIT-Madras, 600 036

Place: Chennai

Date:

ACKNOWLEDGEMENTS

I take pleasure in expressing my profound gratitude to my project guide, Dr. Mahesh Kumar, who gave an opportunity to do this project. His excellent guidance and support throughout the course of my project really made this endeavor a success. It has been a very learning and enjoyable experience to work under his supervision. I am also thankful for the excellent laboratory facilities provided by him in the Power Quality Simulation Laboratory, ESB 342, Department of Electrical Engineering, which facilitated detailed simulation studies concerned to my work.

I deeply appreciate the encouragement extended by my fellow researchers and friends, for sparing time to clarify my doubts. I am particularly thankful to Anvar Hussain, Nafih Muhammed, Manoj Kumar, Nikhil, Sreekanth, Nagesh and Sreenivas for their support during my project. I thoroughly value the discussions with everyone that helped me shape ideas in my mind.

I would like to extend my sincere thanks to my friends for their encouragement and support at the moments of highs and lows in my five years of stay in IIT Madras.

This work would not be what it is, without the encouragement and support from my family members who always stood by my side with strong faith in my decisions. My heartfelt thanks to everyone who may have contributed to this project, directly or indirectly.

Mus-ab.A

ABSTRACT

KEYWORDS: DSTATCOM; Discret wavelet transform; Power quality; Harmonic compensation

With the increasing use of adjustable speed drives, diodes and thyristor rectifiers, computers and their peripherals and other nonlinear devices, harmonic pollution is created in the power distribution system. Such harmonics create more voltage and current stress, electromagnetic interference, more losses, harmonic resonance, etc. The use of induction motors and similar reactive power loads result in poor power factor and hence more line losses in the system. Unevenly distributed loads among the three phases cause increased neutral current in the distribution system. Conventionally These problems are counteracted by the using passive filters. Although the passive filters have the advantages of low cost and losses, they have the problems of harmonic resonance with the source and/or the load. Moreover, they need to be tuned properly to take care of a wider frequency range. In this situation, the promising solution is to use shunt active power filter, also called as distribution static compensator (DSTATCOM) The voltage source inverter (VSI) has to feed the right nature of compensating current for any active power filter (APF). Selection of control strategy for calculating the reference compensator currents plays a vital role in the operation of DSTATCOM. Various methods have been proposed in the literature for harmonic analysis Wavelet Transform (WT) which has certain advantages is preferred. Discrete Wavelet Transform (DWT) is used for the extraction of fundamental frequency component of voltage and current signals. The extracted signal is subtracted from the actual current giving the total harmonic contend present which has to be compensated by DSTATCOM. Discrete Wavelet Transform (DWT) is used to extract the phase information from the analyzed signal. The extracted Phase information is used to detect any sag/swell occurred in voltage and to calculate the reactive power which has to be supplied by the VSI for the power factor improvement. Unbalance in the three phase loads is compensated by applying the concepts of symmetrical components in wavelet domain. Detailed simulation studies and comparison

of results with Complex Wavelet transform are presented. In this project, detection and characterization of power quality disturbances using wavelet transform based technique is discussed. A new strategy for reference currents extraction which utilizes DWT is proposed for compensating major power quality disturbances using DSTATCOM. Simple, fast and non redundant nature of DWT is examined by simulation studies using Matlab/Simulink.

TABLE OF CONTENTS

LIST OF TABLES

LIST OF FIGURES

ABBREVIATIONS

APF	Active Power Filter
CCM	Current Controlled Mode
CWT	Complex Wavelet Transform
DC	Direct Current
DG	Distributed Generation
DSTATCOM	Distribution Static Compensator
DVR	Dynamic Voltage Restorer
DWT	Discrete Wavelet Transform
FFT	Fast Fourier Transform
FT	Fourier Tansform
IDWT	Inverse Discrete Wavelet Transform
IEEE	Institute of Electrical and Electronics Engineers
IGBT	Insulated Gate Bi-polar Transistor
MRA	Multi Resolution Analysis
PCC	Point of Common Coupling
PI	Proportional and Integral
PLL	Phase Locked Loop
PQ	Power Quality
PWM	Pulse Width Modulation
RES	Renewable Energy Sources
SAPF	Shunt Active Power Filter
SRF	Synchronous Reference Frame
STFT	Short Term Fourier Transform
THD	Total Harmonic Distortion
UPQC	Unified Power Quality Conditioner
VCM	Voltage Controlled Mode
VSI	Voltage Source Inverter
WT	Wavelet Transform

NOTATIONS

C_{dc}	DC link capacitance
v_α, v_β, v_0	Instantaneous voltages in $\alpha\beta 0$ frame
v_d, v_q, v_0	Instantaneous voltages in *dq0* frame,
v_{sa}, v_{sb}, v_{sc}	Source voltages in phase a, b and c respectively
v_{la}, v_{lb}, v_{lc}	Three phase load voltages
i_{fa}, i_{fb}, i_{fc}	Three phase shunt inverter current
i_s	Source current
i_{fn}	DSTATCOM neutral current
i_{la}, i_{lb}, i_{lc}	Current drawn by the load
p	Instantaneous active power
q	Instantaneous reactive power
i	Imaginary number
R_s, L_s	Feeder resistance and inductance
R_f, L_f	Shunt inverter filter resistance and inductance
V_{dc}	DC link voltage,
P_{lavg}	Average load power
f_s	Supply frequency
$\bar{g}$	High pass filter for computation of DWT
$\bar{h}$	Low pass filter for computation of DWT
$\bar{V_{dc}}$	DC link voltage
h	Hysteresis band
ω	Frequency
$\psi(t)$	Mother wavelet function
$\phi(t)$	Scaling function
$s(n))$	Approximate coefficient

CHAPTER 1

INTRODUCTION

Quality and reliability of power supply in the distribution system has been gaining importance due to the increased usage of equipments causing disturbances in the system. Power electronic switching devices used in uninterrupted power supply (UPS), switched mode power supply (SMPS), adjustable speed drives (ASDs), uncontrolled rectifiers etc, cause distorted source currents in the distribution system. These non-linear loads along with reactive and unbalanced loads have created an adverse effect on the quality of power supplied by the utility such as large neutral current, overheating of transformer and other electrical equipments,excessive ground to neutral voltage and increased rating of the source. Any fault in the power system results in the PQ issues like voltage sag, swell, unbalances, transients, flicker, etc which in turn cause stoppage or damage of sensitive equipment,malfunction of information technology equipment, namely microprocessor based control systems (PCs, PLCs, ASDs, etc), disconnection and loss of efficiency in electric rotating machines, etc [1].

To alleviate these power quality (PQ) issues, passive filters have been used conventionally [2]. They are basically combination of L and C elements tuned for a particular frequency [3]. Although passive filters have the advantages of low cost and losses,they have the problems of harmonic resonance with the source and/or the load. The compensation characteristics heavily depend on the system impedance because the filter impedance has to be smaller than the source impedance in order to eliminate source current harmonics. Moreover, they need to be tuned properly to take care of a wider frequency range.For eliminating multiple harmonic components, individual filters have to be installed. They are not suitable for variable loads, since, on one hand, they are designed for a specific reactive power, and on the other hand, the variation of the load impedance can detune the filter. Overloads can happen in the passive filter due to the circulation of harmonics coming from nonlinear loads connected near the connection point of the passive filter [5]. These difficulties make the passive filter less attractive and use of active power filters becomes important in this scenario.

1.1 Active Power Filters

Active filters are simply power electronic converters, specifically designed to inject harmonic current with equal magnitude and opposite phase. This idea was proposed during 1970s, but because of the technological limitation in power system and signal processing units, it was not brought into practice during those periods. In recent years, active power filters have been researched and developed to compensate harmonics generated by static power converters and large capacity power apparatus [4]. Attention has been paid to the active power filter using switching devices such as power transistors, gate turn-off (GTO) thyristors, and static induction (SI) thyristors, which have made remarkable progress in capacity and switching performance. The concept was implemented using Insulated Gate Bipolar Transistors (IGBT) and new generation digital signal processors (Akagi,1994). Active power filters can compensate the wider range of harmonics as well as the reactive power required for the load. The basic functions of active filters can be summarized as,

- Eliminating voltage and current harmonics
- Reactive power compensation
- Regulating terminal voltage
- Compensating the voltage flickering
- Improving voltage balance in three-phase systems

The active filter can be divided into a power circuit and signal circuit. The power circuit produces the required current or voltage to be injected into the point of common coupling (PCC). The main component of a power circuit is a voltage source inverter (VSI) with a dc storage capacitor. The VSI is made of power electronic switches such as IGBT. The signal circuit provides the required switching pulses for the VSI. The VSI is connected to the system through a coupling inductor.

The wide range of objectives of active filter can be achieved either individually or in combination, depending upon the requirements and control strategy and configuration which have to be selected appropriately [6].

1.2 Classification of Active Filters

Based on topology, the active power filters are classified as follows

- Shunt active power filter
- Series active power filter
- Hybrid power filter
- Unified power quality conditioner (UPQC)

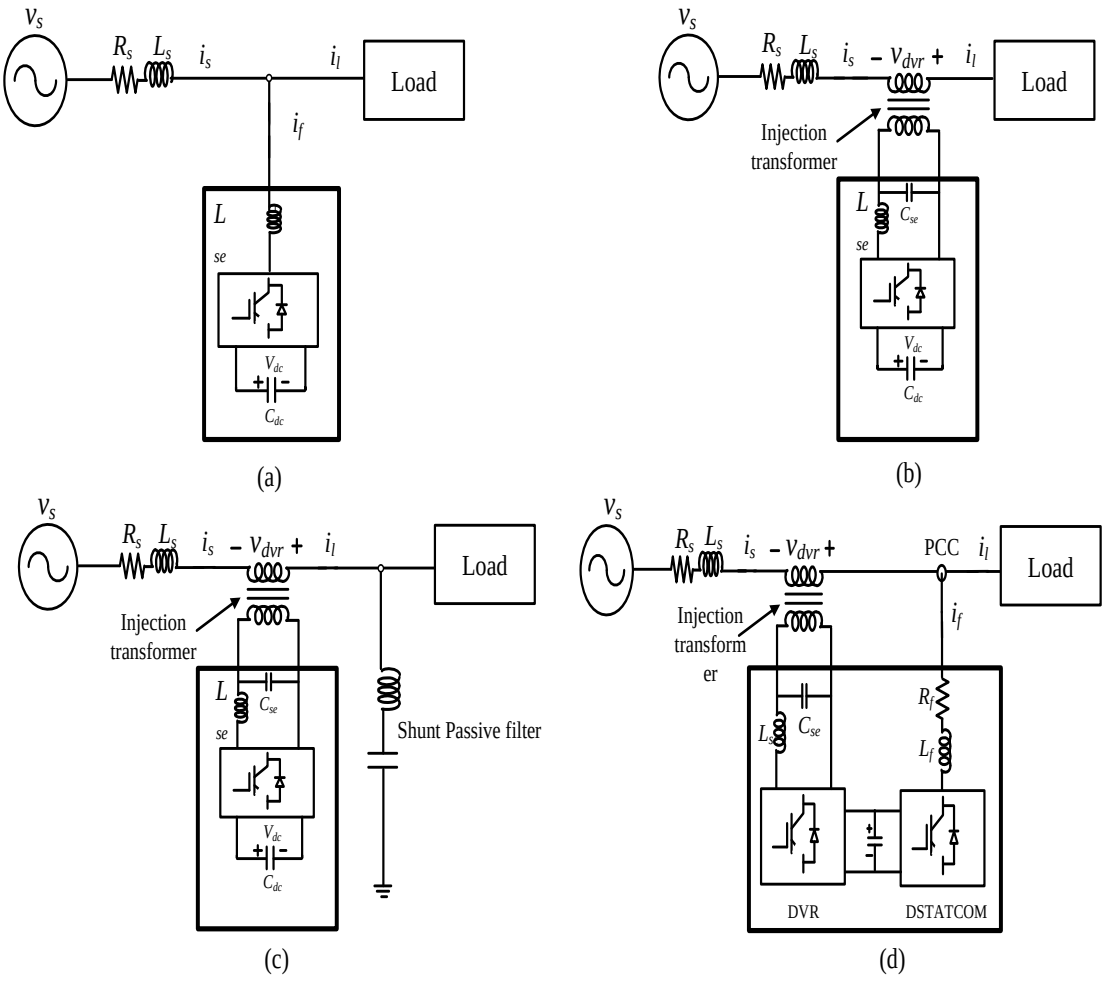

Figure 1.1: Schematic diagram of (a) Shunt active power filter (b) Series active power filter (c) Series active and shunt passive power filter (d) Unified power quality conditioner.

1.2.1 Shunt Active Power Filter

The APF connected in shunt with the load bus is called as distribution static compensator (DSTATCOM). It has been introduced as a solution to overcome the power quality

problems caused by nonlinear reactive and unbalanced loads [7]. Schematic diagram of DSTATCOM is shown in Fig. 1.1(a). It consists of a voltage source inverter (VSI) operated in either current control mode (CCM) or voltage control mode (VCM), supported by dc link capacitor (C_{dc}) which keeps the DC voltage constant and acts as a storage device to provide real power difference between load and source during transient. Compensation current is injected through interfacing filter (L_f) connected at the point of common coupling (PCC). When the VSI is operated in CCM, DSTATCOM supplies reactive, harmonics, and unbalances in the load currents to make source currents balanced, sinusoidal and in-phase with the respective phase voltages.

1.2.2 Series Active Power Filter

The APF connected in series with the feeder is called as dynamic voltage restorer (DVR). Schematic diagram of DVR is shown in Fig. 1.1(b). It consists of a VSI, a series injection transformer, and a passive filter (L_{se} and C_{se}) to eliminate high switching frequency component of VSI [8]. The series interconnection is required to allow the injected voltage by the series transformer to add to the utility system voltage. The sum of the line voltage and the inserted voltage becomes the restored voltage seen by the critical load.

1.2.3 Hybrid Active Filter

Advantages of both active filter and passive filter can be combined by using a hybrid active power filter. Since the active power filter requires higher voltage/current switches for medium/high power applications, hybrid filter is introduces to address this issue [9]. Several configurations of hybrid active filter have been proposed [10]-[11]. One such a configuration is given in Fig. 1.1(c). In hybrid filter, a lower rating active filter is added in series with the passive filter, having the merit of operating the active filter at a convenient voltage and current [12].

1.2.4 Unified Power Quality Conditioner

Unified power quality conditioner (UPQC) is a combination of series and shunt active power filters. Schematic diagram of UPQC is shown in Fig. 1.1(d). UPQC has the capability to compensate supply voltage flicker, sag, swell, load reactive power, voltage and current unbalance and harmonics in voltage and current. It consists of a control unit and power circuit. Voltage and current disturbance detection, reference signal generation, gate pulse generation and voltage/current measurement are done by control unit. Power circuit consists of two VSI, standby and system protection systems, injection transformers and harmonic filters. Though UPQC is considered as one of the most powerful equipment to mitigate all the power quality issues, it has the main drawback of large cost and control complexity because of the more number of solid state devices involved.

1.3 Motivation

From the above discussions, it is clear that various power conditioning devices have been proposed in order to mitigate the power quality issues. Among the various choices available in devices, DSTATCOM is chosen as the compensating device due to the less control complexity and cost compared to other devices. The main aspects in the realization of the DSTATCOM are

- control strategy selection for generation of reference currents to the compensator
- selection of suitable topology for Voltage Source Inverter (VSI)
- selection of switching control strategy for the VSI to realize the compensator currents

Out of these aspects, this thesis focuses on the selection of control strategy for the compensator. One of the major part of any active filter set up is the control algorithm to calculate the instantaneous value of reference signal. The algorithm should have good steady state and transient response. The present work focuses on the control algorithm for DSTATCOM. Most of the control algorithms available in the literature are time domain based methods and fail at certain disturbances such as system frequency variation, unequal disturbances in all phases etc. This project proposes a new control algorithm for DSTATCOM, which addresses these issues.

1.4 Objectives and Scope

The main areas focused in this project are detection and estimation of power quality disturbances and power quality enhancement using DSTATCOM in a distribution system. Following are the objectives of this research work:

- A suitable reference current generation algorithm needs to be explored for the DSTATCOM, which can exhibit additional advantages as compared to conventional methods. The new method should allow DSTATCOM to tackle power quality issues by providing power factor correction, harmonic elimination and load balancing based on the load requirement.
- Huge advancements achieved in the computing technology and information theory need to be utilized in order to mitigate the power quality disturbances. Taking advantages of newly emerging Wavelet Transform based techniques, which could be used as a complete solution for the power quality issues, a novel control algorithm has to be developed.
- Based on Wavelet Transform, an algorithm has to be developed for accurate estimation of voltage and current harmonics. The developed method should have less computational burden for real-time implementation in a digital signal processor.
- WT based methods have been used only for the detection and classification of power quality disturbances and compensation of harmonics In addition to these, possibilities of compensation of reactive power as well as unbalances in load have to be explored.
- Validation of WT based methods has to be conducted using online simulation studies.

1.5 Organization of the Thesis

Chapter 1 explains different power filters used in the power distribution system. A brief description of structure and classification and comparison of various power filters have been presented in this chapter. Finally, motivations and objectives of the thesis are explained.

Chapter 2 provides a detailed literature survey of various power quality issues commonly occurring in the distribution system. Design and structure of DSTATCOM have been discusses in detail and different time based reference quantity generation algorithms are also presented in this chapter.

Chapter 3 given an introduction to the vast wavelet analysis. Mathematical aspects of wavelet analysis are discussed and a brief comparison of Discrete and Continuous Wavelet Transform has been made in this chapter. Advantages and applications of wavelet analysis in power quality area are presented in detail.

Chapter 4 discusses proposed wavelet based reference current generation techniques. The new algorithm can be used for the harmonic compensation and phase extraction of sinusoid waveforms. The proposed method is compared with the existing methods and accuracy of the proposed method is discussed. Positive sequence extraction of the extracted fundamental is done using wavelet technique and load unbalances are compensated this extracted waveform.

Chapter 5 discusses the simulation results. The performance of the proposed algorithm for the DSTATCOM is verified with the help of simulation results.

Chapter 6 discusses the conclusion and future scope of work.

CHAPTER 2

LITERATURE REVIEW

Power quality has emerged as a topical issue in power systems in the 1990s when it started to influence the working of high technology equipments related to automation, communication, process control and precise manufacturing technique. The recent thrust on extracting power from renewable energy sources (RESs) calls for extensive studies on power filters to make the renewable energy green and clean (i.e., free from harmonics). Introduction of strict legislation such as IEEE519 limits the maximum amount of harmonics that a supply system can tolerate for a particular type of load [13]. Therefore development of more sophisticated instruments for measuring power quality disturbances and the use of new methods in processing and analyzing the measurements became essential. Fourier theory has been the core of many traditional techniques and it is still widely used today. However, it is increasingly being replaced by newer approaches notably wavelet transform and especially in the post-event processing of the time-varying phenomena. This project reviews the use of wavelet transform approach in processing power quality data using DSTATCOM. Different power quality terms, DSTATCOM configurations and control methods are briefly described in this chapter

2.1 Power Quality Issues

Power quality issues can be divided into two broad categories of time-varying and steady-state (or intermittent) events. Time varying events include

- Voltage transients
- Dips
- Swells
- Interruptions

They normally occur for a brief period of time (several milliseconds), but are often severe enough to cause fatal disruptions to many electrical loads. Voltage dips lasting

5-6 cycles are known to cause malfunction to programmable logic controller (PLC) in factories.

Steady state events include

- Voltage unbalances
- Harmonic and interharmonic distortions
- Voltage fluctuation
- Notching
- Noise

These steady-state phenomena would act subtly over a certain period of time before intolerable condition surfaces. Harmonic voltage causes additional stress on equipment insulation which results in shortening of their useful life. The eventual insulation breakdown often occurs after the equipment is being subjected to the distortion over extended period of time.

2.1.1 Voltage Transient

Voltage transient is said to have occurred when the voltage varies rapidly between two consecutive steady states for short duration of time. It can be a unidirectional impulse of either polarity or a damped oscillatory wave with the first peak occurring in either polarity. Transients are categorized as either impulse or oscillatory. Impulse transients typically have a fast rise time, a fairly rapid decay, and a high energy content, rising to hundreds and even thousands of volts. Their duration can be from a few microseconds up to 200 microseconds. Oscillatory transient has a fast rise time, oscillations that decay exponentially, and lower energy content than impulse transients (250 V to 2,500 V).

2.1.2 Voltage Sag

Voltage sag is the decrease in normal voltage level between 10 and 90 percent of nominal voltage for one-half cycle to one minute [13]. It is usually associated with faults in consumers' installation or distribution network, starting of heavy motors and switching of large loads. It results in the malfunction of microprocessor based systems like PCs, PLCs, ASDs and disconnection and loss of efficiency in electric rotating machines.

2.1.3 Voltage Swell

Voltage swell is the increase in rms voltage at the power frequency for durations from 0.5 cycles to 1 min [13]. It is associated with system faults such as line to ground faults and large load switching off and a capacitor bank switching on. Swell duration is subdivided into three categories, namely instantaneous, temporary, and momentary which coincide with the three categories of sag and interruption.

2.1.4 Interruption

It is classified by IEEE 1159 into either a short-duration or long-duration variation (Sustained interruptions). They are measured and described by their duration since the voltage magnitude is always less than 10 per cent of nominal. Short-duration interruption is defined as the decrease in the voltage supply level to less than 10 percent of nominal for up to one minute duration [13]. It results from re-closing of circuit breakers or reclosers attempting to clear non-permanent faults, first opening and then re-closing after a short time delay. Long duration interruption is defined as the decrease in the voltage supply level to zero for more than one minute. Sustained interruptions are often permanent in nature and require manual intervention for restoration. These interruptions are usually caused by permanent faults due to storms, trees striking lines or poles, utility or customer equipment failure in the power system or misco-ordination of protection devices. Consequently, such disturbances would result to a complete shutdown of the customer facility.

2.1.5 Voltage Unbalances

Voltage Unbalance is defined by IEEE as the ratio of the negative or zero sequence component to the positive sequence component [13]. In simple terms, it is the voltage variation in three phase system in which the three voltage magnitudes or the phase angle differences between them are not equal. It follows that this power quality problem affects only poly-phase systems (e.g. three-phase). The utility can be the source of unbalanced voltages due to malfunctioning equipment, including blown capacitor fuses, open-delta regulators, and open-delta transformers. It can also be caused by uneven

single-phase load distribution among the three phases - the likely culprit for a voltage unbalance of less than 2%. The main effect of voltage unbalance is motor damage from excessive heat. Voltage unbalance can create a current unbalance 6 to 10 times the magnitude of voltage unbalance. Unbalance in the system implies the existence of negative sequence that is harmful to all three phase loads.

2.1.6 Harmonic Distortions

Harmonics are described by IEEE as sinusoidal voltages or currents having frequencies that are integer multiples of the fundamental frequency at which the power system is designed to operate. Harmonic distortion levels can be characterized by the complete harmonic spectrum with magnitudes and phase angles of each individual harmonic component. Total Harmonic Distortion (THD) is also common to use as a measure of the effective value of harmonic distortion. They exist due to the nonlinear characteristics loads and devices on the electrical power system. Electric machines working above the knee of the magnetization curve (magnetic saturation), arc furnaces, welding machines, rectifiers, and DC brush motors also inject harmonic components into the system. It has become an increasing concern for many end-users and for the overall power system because of the growing application of power electronics equipment. Harmonics primarily result in the significant overheating of equipment, cables and wires. High harmonic level in the system causes neutral overload in 3-phase systems, electromagnetic interference with communication systems and loss of efficiency in electric machines, increased probability in occurrence of resonance

2.1.7 Voltage Fluctuation

Voltage Fluctuations are described by IEEE as systematic variations of the voltage waveform envelope, or a series of random voltage changes, the magnitude of which falls between the voltage limits set by ANSI C84.1. The most important effect of this power quality problem is the variation in the light output of various lighting sources, commonly termed as Flicker. Voltage fluctuations are generally caused by loose or corroded connections at either the house or on the power lines, and are often noticed by flickering lights.Equipment or devices that exhibit continuous, rapid load current vari-

ations (mainly in the reactive component) can also cause voltage fluctuations and light flicker. It can affect the production environment by causing personnel fatigue and lower work concentration levels. In addition, voltage fluctuations may subject electrical and electronic equipment to detrimental effects that may disrupt production processes with considerable financial costs.

2.1.8 Notching

Voltage notching is described as a recurring power quality disturbance due to the normal operation of power electronic devices (i.e. rectifier), when current is commutated from one phase to another. It is primarily caused by three-phase rectifiers or converters that generate continuous DC current. Voltage Notches introduce harmonic and non-harmonic frequencies that are much higher than those found in higher voltage systems. Since these frequencies are in the radio frequency range, they cause negative operational effects, such as signal interference introduced into logic and communication circuits. In addition, the voltage notching effect may overload electromagnetic interference filters, and other similar high-frequency sensitive capacitive circuits.

2.1.9 Noise

Noise is defined as the unwanted electrical signals with broadband spectral content superimposed on the waveform of power system frequency. Television diffusion, radiation due to welding machines, electromagnetic interference due to microwaves, control circuits and switching power supplies can cause noise in the power system. Improper grounding can also be the reason of noise. It causes disturbances on the sensitive equipments, data loss and data processing errors.

2.2 DSTATCOM - Design and Control

Various power quality problems have been discussed in section 2.1. DSTATCOM can be used to mitigate both current and voltage related power quality problems based on the mode of operation. This project focuses on the mitigation of current related issues

using DSTATCOM by operating it in current controlled mode (CCM).

2.2.1 Structure and Operation of DSTATCOM

The power circuit diagram of a three phase four wire neutral point clamped VSI topology based DSTATCOM connected in a distribution system is given in Fig. 2.1. In this figure, v_{sa}, v_{sb} and v_{sc} are source voltages of phases a, b and c, respectively. The loads, source, and compensator together are connected at the PCC. The source currents in three phase are represented by i_{sa}, i_{sb} and i_{sc}, load currents are represented by i_{la}, i_{lb} and i_{lc}. The VSI currents are denoted by i_{fa}, i_{fb}, i_{fc} in respective phases. The interfacing inductance and resistance of the shunt active filter are represented by L_f and R_f respectively. The shunt capacitor (C_f), connected at the load terminal, absorbs the higher switching harmonics present in the filter currents. The dc link capacitor keeps the DC voltage constant and acts as a storage device to provide real power difference between load and source during transient [14].

2.2.2 DC Capacitance (C_{dc})

The value of DC capacitor is determined either based on the instantaneous energy-balance concept, or on the mitigation oscillations possibility of continuous bus voltage imposed by the lower order harmonics or unbalanced of linear/non-linear loads [22].

The capacitor needs to supply the real power demand of the load until the capacitor voltage controller comes into action. This transfer of real power during the transient will result in deviation of capacitor voltage from its reference value. Let E_{max} be the maximum energy that the capacitor has to supply in the worst case of transient. This energy will be equal to change in the capacitor stored energy. Therefore,

$$\frac{1}{2}C_{dc}\left(V_{dcref}^2 - V_{dc}^2\right) = E_{max} \tag{2.1}$$

where V_{dcref} and V_{dc} are reference dc bus voltage and maximum allowed voltage during transients respectively. Consider the voltage controller takes p cycles i.e., $p\,T$ seconds to act, where T is system time period. Let total load rating is S kVA. Hence, maximum

energy exchange by compensator during transient will be $p\,S\,T$. Hence

$$C_{dc} = \frac{2\,p\,S\,T}{V_{dcref}^2 - V_{dc}^2}. \tag{2.2}$$

2.2.3 Filter Inductance(L_f)

The value of the filter inductance is chosen such that it should allow a high rate of change of current to all harmonics, and limit higher frequency switching components. A compromised value is determined from the constraint on the maximum ripple current, $\Delta I_{\ (p-p)\ max}$. In a six-switch converter, the maximum ripple current occurs at the zero-crossings of the fundamental frequency component of the output voltage. Hence the inductance can be calculated as:

$$L_f = \frac{V_{dc}}{6 f_s \Delta I_{(p-p)\max}} \tag{2.3}$$

Objective of the DSTATCOM in CCM is to inject the appropriate fundamental reactive current to

- Compensate the load harmonic currents to make source currents sinusoidal.
- Compensate the reactive component of load currents to make power factor at the PCC unity.
- Compensate load unbalance to make source neutral current zero.

DSTATCOM can inject either leading or lagging fundamental reactive current to maintain the load voltage constant. If the source voltage decreases, DSTATCOM acts like a capacitor load and injects reactive current. If the source voltage increases, DSTATCOM acts as an inductor and draws the reactive current from the source to improve the load voltage.

2.3 Reference Quantity Generation Strategies for DSTATCOM

Control strategy for the generation of reference quantities determines the desired operation and behavior of DSTATCOM. There are several power theories available in the

existing literature [15]-[21] Most commonly used theories include

- Instantaneous reactive power theory [16]-[18]
- Synchronous reference theory [23]
- Instantaneous symmetrical components theory [21]

2.3.1 Instantaneous Reactive Power Theory

Instantaneous reactive power theory was proposed by Akagi et.al. in 1983-84 and is also called *pq* theory. This theory aims at developing a mathematical formulation for the realization of reference currents using instantaneous reactive power in the load. Instantaneous values of voltage and current are used to calculate he compensating quantities. Clarke transformation has been used to transform the *abc* phase voltages and currents to the stationary α - β axis as given in Fig. 2.2 and represented by following equation:

$$\begin{bmatrix} v_\alpha \\ v_\beta \\ v_0 \end{bmatrix} = \sqrt{\frac{2}{3}} \begin{bmatrix} 1 & -\frac{1}{2} & -\frac{1}{2} \\ 0 & \frac{\sqrt{3}}{2} & -\frac{\sqrt{3}}{2} \\ \frac{1}{\sqrt{2}} & \frac{1}{\sqrt{2}} & \frac{1}{\sqrt{2}} \end{bmatrix} \begin{bmatrix} v_a \\ v_b \\ v_c \end{bmatrix} ; \begin{bmatrix} i_\alpha \\ i_\beta \\ i_0 \end{bmatrix} = \sqrt{\frac{2}{3}} \begin{bmatrix} 1 & -\frac{1}{2} & -\frac{1}{2} \\ 0 & \frac{\sqrt{3}}{2} & -\frac{\sqrt{3}}{2} \\ \frac{1}{\sqrt{2}} & \frac{1}{\sqrt{2}} & \frac{1}{\sqrt{2}} \end{bmatrix} \begin{bmatrix} i_a \\ i_b \\ i_c \end{bmatrix}. \quad (2.4)$$

The instantaneous real power is defined as product of instantaneous voltage on one axis and instantaneous current on the same axis, is given as

$$p = v_\alpha i_\alpha + v_\beta i_\beta. \quad (2.5)$$

The instantaneous reactive power is defined as cross product of the instantaneous voltage in one axis and the instantaneous current in the other axis, given as

$$q = \vec{v}_\alpha \times \vec{i}_\beta + \vec{v}_\beta \times \vec{i}_\alpha = v_\alpha i_\beta - v_\beta i_\alpha. \quad (2.6)$$

Using (2.4) and (2.6), instantaneous reactive power in *abc* coordinates is given as

$$q = -\frac{1}{\sqrt{3}}[(v_a - v_b)i_c + (v_b - v_c)i_a + (v_c - v_a)i_b] = -\frac{1}{\sqrt{3}}[v_{ab}i_c + v_{bc}i_a + v_{ca}i_b]. \quad (2.7)$$

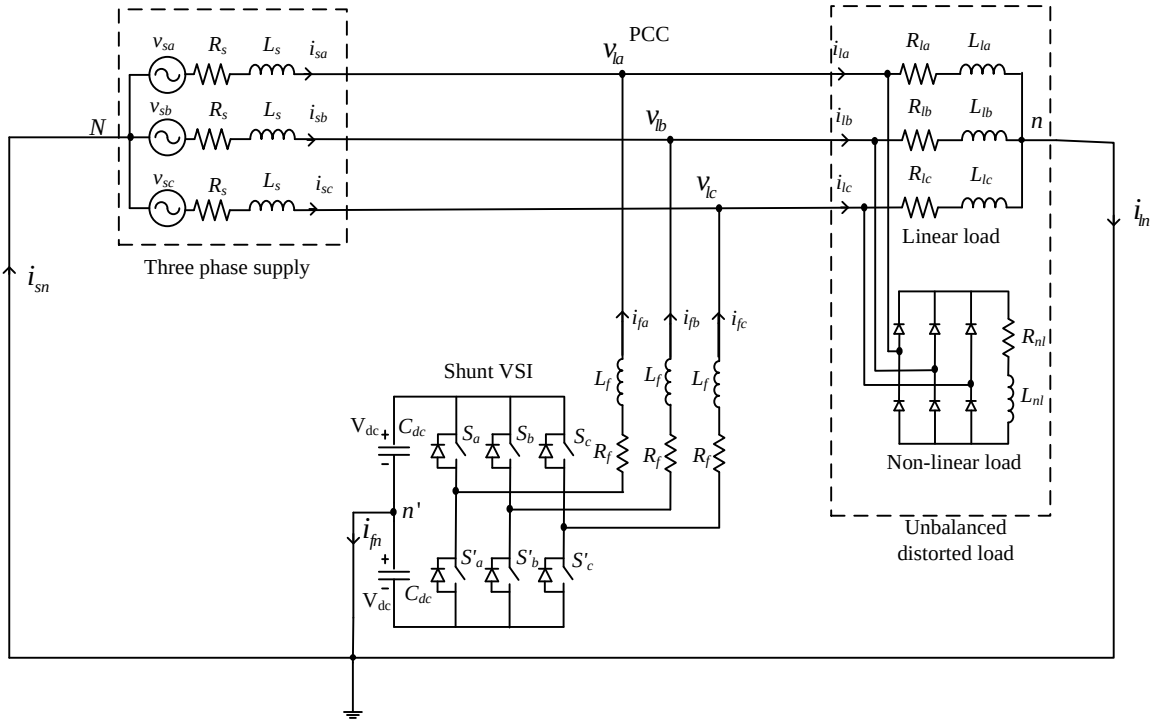

Figure 2.1: Power circuit diagram of DSTATCOM.

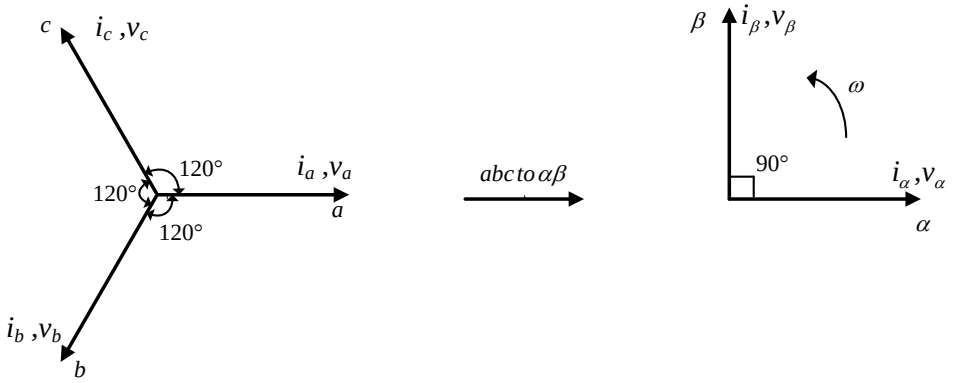

Figure 2.2: *abc* to $\alpha\beta$ transformation.

From (2.5) and (2.6), instantaneous real and reactive powers in $\alpha\beta$- coordinates can be expressed in the following matrix form:

$$\begin{bmatrix} p \\ q \end{bmatrix} = \begin{bmatrix} v_\alpha & v_\beta \\ -v_\beta & v_\alpha \end{bmatrix} \begin{bmatrix} i_\alpha \\ i_\beta \end{bmatrix}. \tag{2.8}$$

(2.8) is arranged as follows:

$$\begin{bmatrix} i_\alpha \\ i_\beta \end{bmatrix} = \begin{bmatrix} v_\alpha & v_\beta \\ -v_\beta & v_\alpha \end{bmatrix}^{-1} \begin{bmatrix} p \\ q \end{bmatrix} = \frac{1}{v_\alpha^2 + v_\beta^2} \begin{bmatrix} v_\alpha & -v_\beta \\ v_\beta & v_\alpha \end{bmatrix} \begin{bmatrix} p \\ q \end{bmatrix} = \begin{bmatrix} i_{\alpha p} \\ i_{\beta p} \end{bmatrix} + \begin{bmatrix} i_{\alpha q} \\ i_{\beta q} \end{bmatrix}. \tag{2.9}$$

where:

α- axis instantaneous active current $i_{\alpha p}$ = $v_\alpha p/(v_\alpha^2 + v_\beta^2)$

α- axis instantaneous reactive current $i_{\alpha q}$ = $-v_\beta q/(v_\alpha^2 + v_\beta^2)$

β- axis instantaneous active current $i_{\beta p}$ = $v_\beta p/(v_\alpha^2 + v_\beta^2)$

β- axis instantaneous reactive current $i_{\beta q}$ = $v_\alpha q/(v_\alpha^2 + v_\beta^2)$.

The instantaneous power in the α - axis and β - axis are defined as follows:

$$\begin{bmatrix} p_\alpha \\ p_\beta \end{bmatrix} = \begin{bmatrix} v_\alpha i_\alpha \\ v_\beta i_\beta \end{bmatrix} = \begin{bmatrix} v_\alpha i_{\alpha p} \\ v_\beta i_{\beta p} \end{bmatrix} + \begin{bmatrix} v_\alpha i_{\alpha q} \\ v_\beta i_{\beta q} \end{bmatrix}. \tag{2.10}$$

$$p = \frac{v_\alpha^2}{v_\alpha^2 + v_\beta^2}\, p + \frac{v_\beta^2}{v_\alpha^2 + v_\beta^2}\, p + \frac{-v_\alpha v_\beta}{v_\alpha^2 + v_\beta^2}\, q + \frac{v_\alpha v_\beta}{v_\alpha^2 + v_\beta^2}\, q. \tag{2.11}$$

$$p = p_{\alpha p} + p_{\beta p} + p_{\alpha q} + p_{\beta q} = p_\alpha + p_\beta \tag{2.12}$$

where

α- axis instantaneous active power $p_{\alpha p}$ = $v_\alpha^2 p/(v_\alpha^2 + v_\beta^2)$

α- axis instantaneous reactive power $p_{\alpha q}$ = $-v_\alpha v_\beta q/(v_\alpha^2 + v_\beta^2)$

β- axis instantaneous active power $p_{\beta p}$ = $v_\beta p/(v_\beta^2 + v_\beta^2)$

β- axis instantaneous reactive power $p_{\beta q}$ = $v_\alpha v_\beta q/(v_\alpha^2 + v_\beta^2)$.

Using (2.8), the filter current components in terms of its powers and voltages can be expressed as in the following:

$$\begin{bmatrix} i_{f\alpha}^* \\ i_{f\beta}^* \end{bmatrix} = \begin{bmatrix} v_\alpha & v_\beta \\ -v_\beta & v_\alpha \end{bmatrix}^{-1} \begin{bmatrix} p_f \\ q_f \end{bmatrix} \tag{2.13}$$

where $i_{f\alpha}^*$ and $i_{f\beta}^*$ are the reference filter currents, p_f and q_f are the powers to be compensated. Instantaneous active and reactive powers p and q can be decomposed into an average and an oscillatory component. $p = \bar{p} + \tilde{p}$ and $q = \bar{q} + \tilde{q}$. The terms $\bar{p}$ and $\tilde{p}$ are the average and oscillatory components of the p, whereas $\bar{q}$ and $\tilde{q}$ are the average and oscillatory components of the q.

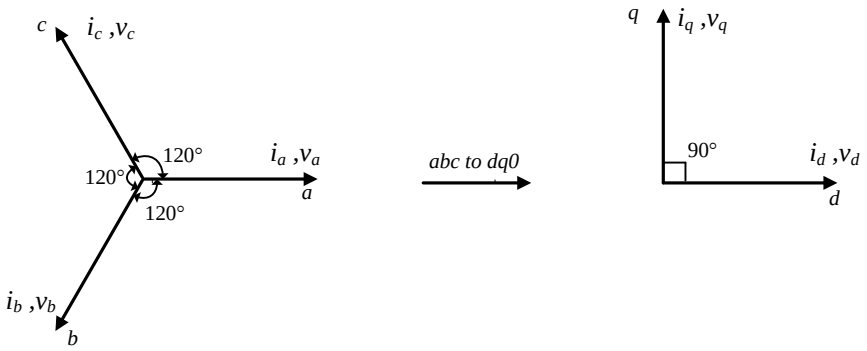

Figure 2.3: abc to dqo transformation.

By selecting $p_f = \tilde{p}$ and $q_f = \bar{q} + \tilde{q}$, the instantaneous harmonic active current, instantaneous fundamental reactive current and instantaneous harmonic reactive current can be compensated. Because of the instantaneous reactive currents, the displacement factor is unity in both steady state and transient states.

2.3.2 Synchronous Reference Frame Theory

The synchronous reference frame (SRF) theory or dq theory is based on the transformation of currents in synchronously rotating dq frame. The basic structure of SRF controller consists of direct dq and inverse dq Park transformations. The reference frame transformation is formulated from a three phase *abc* stationary system to the direct axis (d) and quadratic axis (q) rotating coordinate system. The three phase space vectors stationary coordinates are transformed into two axis $dq0$ rotating reference frame transformation as following:

$$\begin{bmatrix} v_d \\ v_q \\ v_0 \end{bmatrix} or \begin{bmatrix} i_d \\ i_q \\ i_0 \end{bmatrix} = \sqrt{\frac{2}{3}} \begin{bmatrix} \cos(\omega t) & \cos(\omega t - 2\pi/3) & \cos(\omega t + 2\pi/3) \\ -\sin(\omega t) & -\sin(\omega t - 2\pi/3) & -\sin(\omega t + 2\pi/3) \\ \frac{1}{\sqrt{2}} & \frac{1}{\sqrt{2}} & \frac{1}{\sqrt{2}} \end{bmatrix} \begin{bmatrix} v_a \\ v_b \\ v_c \end{bmatrix} or \begin{bmatrix} i_a \\ i_b \\ i_c \end{bmatrix}. \tag{2.14}$$

Similarly we can do this for the current also. Voltage signals are processed by a phase-locked loop (PLL) to generate unit voltage templates (sine and cosine signals). The PLL circuit provides the rotation speed (rad/sec) of the rotating reference frame, where ωt is set as fundamental frequency component. Current signals are transformed to dq frame, where these signals are filtered and transformed back to abc frame (i_{sa},i_{sa},

and i_{sc}), which are fed to a hysteresis-based PWM signal generator [12] to generate final switching signals fed to the DSTATCOM. Depending on the fundamental, harmonics and negative sequence components in voltages and currents, the dq components can have different frequencies. The analysis of the dq components and appropriate filtering can support the generation of the current and voltage references as required by the control. The dq components consisting of DC and AC components are given as following:

$$i_{Ld} = \bar{i}_{Ld} + \tilde{i}_{Ld},\ i_{Lq} = \bar{i}_{Lq} + \tilde{i}_{Lq}. \tag{2.15}$$

The DC components $\bar{i}_{Ld}$ and $\bar{i}_{Lq}$ correspond to the fundamental positive sequence load currents and the AC components $\tilde{i}_{Ld}$ and $\tilde{i}_{Lq}$ correspond to the load currents harmonics. Component $\bar{i}_{Lq}$ corresponds to the reactive power drawn by the load. The reference for the compensator can be obtained as follows:

$$i^*_{fd} = -\tilde{i}_{Ld},\ i^*_{fq} = -\bar{i}_{Lq} - \tilde{i}_{Lq},\ i^*_{f0} = -i_{L0}. \tag{2.16}$$

The shunt active filter references in abc reference frame are obtained as follows:

$$\begin{bmatrix} i^*_{fa} \\ i^*_{fb} \\ i^*_{fc} \end{bmatrix} = \sqrt{\frac{2}{3}} \begin{bmatrix} \cos(\omega t) & -\sin(\omega t) & \frac{1}{\sqrt{2}} \\ \cos(\omega t - 2\pi/3) & -\sin(\omega t - 2\pi/3) & \frac{1}{\sqrt{2}} \\ \cos(\omega t + 2\pi/3) & -\sin(\omega t + 2\pi/3) & \frac{1}{\sqrt{2}} \end{bmatrix} \begin{bmatrix} i^*_{fd} \\ i^*_{fq} \\ i^*_{f0} \end{bmatrix}. \tag{2.17}$$

The calculation of reference currents using this approach is not affected by voltage unbalance or/and distortion. However, PLL is used in this method to obtain the transformation angle (ωt) from the supply voltage, so this will affect the performance when the supply voltages are unbalanced or/and distorted. This method involves complex transformations and its implementation in DSP is also difficult.

2.3.3 Instantaneous Symmetrical Components Theory

The theory of instantaneous symmetrical components can be used for load balancing, harmonic suppression and power factor correction. Control algorithm based on this

theory can partially or fully compensate any kind of unbalance and harmonic in the load with high bandwidth current sources to track the filter reference currents. According to symmetrical component theory, any three phase instantaneous quantities can be expressed into positive, negative and zero sequence using the following equation.

$$\begin{bmatrix} \boldsymbol{i}_{sa}^{0} \\ \boldsymbol{i}_{sa}^{+} \\ \boldsymbol{i}_{sa}^{-} \end{bmatrix} = \frac{1}{3} \begin{bmatrix} 1 & 1 & 1 \\ 1 & a & a^2 \\ 1 & a^2 & a \end{bmatrix} \begin{bmatrix} i_{sa} \\ i_{sb} \\ i_{sc} \end{bmatrix} ; \begin{bmatrix} \boldsymbol{v}_{sa}^{0} \\ \boldsymbol{v}_{sa}^{+} \\ \boldsymbol{v}_{sa}^{-} \end{bmatrix} = \frac{1}{3} \begin{bmatrix} 1 & 1 & 1 \\ 1 & a & a^2 \\ 1 & a^2 & a \end{bmatrix} \begin{bmatrix} v_{sa} \\ v_{sb} \\ v_{sc} \end{bmatrix}. \tag{2.18}$$

In (2.18), $+$, $-$ and 0, indicates positive, negative and zero sequence components respectively. The quantity 'a' is a complex operator and is equal to e^{j120^0}. It is to be noted that the instantaneous positive sequence ($\boldsymbol{i}_{sa}^{+}$) and the negative sequence ($\boldsymbol{i}_{sa}^{-}$) are complex conjugates of each other and the zero sequence component ($\boldsymbol{i}_{sa}^{0}$) is a real quantity which is zero if the currents are balanced. Like pq theory, we assume that the supply voltages are balanced.

In a three phase four wire system, supply currents should be balanced i.e., neutral current will be zero. Therefore,

$$i_{sa} + i_{sb} + i_{sc} = 0. \tag{2.19}$$

The angle between the positive sequence components of the source current ($\boldsymbol{i}_{sa}^{+}$) and the source voltage ($\boldsymbol{v}_{sa}^{+}$) is same as the power factor angle (φ^{+}) between the balanced source currents and voltages. This power factor angle can be explicitly set to any desired value in the control algorithm. However, it is not directly expressed in the pq theory described earlier. If we now assume that the phase of the $\boldsymbol{i}_{sa}^{+}$ lags that of $\boldsymbol{v}_{sa}^{+}$ by an angle (φ^{+}), we get

$$\angle\{v_{sa} + a v_{sb} + a^2 v_{sc}\} = \angle\{i_{sa} + a i_{sb} + a^2 i_{sc}\} + \varphi^{+}. \tag{2.20}$$

Equation (2.20) is expanded after substituting the values for a and a^2, it is given as follows:

$$\angle\left\{(v_{sa} - \frac{1}{2}v_{sb} - \frac{1}{2}v_{sc}) - j\frac{\sqrt{3}}{2}(v_{sb} - v_{sc})\right\} = \angle\left\{(i_{sa} - \frac{1}{2}i_{sb} - \frac{1}{2}i_{sc}) - j\frac{\sqrt{3}}{2}(i_{sb} - i_{sc})\right\} + \varphi^{+}. \tag{2.21}$$

Equating the angles, we can write (2.21) as follows:

$$\tan^{-1}(K_1/K_2) = \tan^{-1}(K_3/K_4) + \varphi^+ \tag{2.22}$$

where

$$K_1 = \frac{\sqrt{3}}{2}(v_{sb} - v_{sc}) \qquad K_2 = (v_{sa} - \frac{1}{2}v_{sb} - \frac{1}{2}v_{sc})$$
$$K_3 = \frac{\sqrt{3}}{2}(i_{sb} - i_{sc}) \qquad K_4 = (i_{sa} - \frac{1}{2}i_{sb} - \frac{1}{2}i_{sc}).$$

Taking tangents on both sides of (2.22), we get

$$\frac{K_1}{K_2} = \tan\left[\tan^{-1}(K_3/K_4) + \varphi^+\right] = \frac{K_3/K_4 + \tan\ \varphi^+}{1 - (K_3/K_4)\tan\ \varphi^+}. \tag{2.23}$$

Substituting values of K_1, K_2, K_3 and K_4 in (2.23), we get

$$\begin{aligned}(v_{sb} - v_{sc} - 3\gamma(v_{sa} - v_0))i_{sa} + (v_{sc} - v_{sa} - 3\gamma(v_{sb} - v_0))i_{sb} + \\ (v_{sa} - v_{sb} - 3\gamma(v_{sc} - v_0))i_{sc} = 0\end{aligned} \tag{2.24}$$

where $\gamma \equiv \tan\varphi^+/\sqrt{3}$. For unity power factor φ^+ = 0, hence $\gamma = 0$. It is well known that the instantaneous power in a balanced three phase circuit is constant while for an unbalanced circuit it has a double frequency component in addition to the DC or mean value. The presence of harmonics adds higher frequency oscillating component of the instantaneous power. The objective of the compensator is to supply the oscillating component of the instantaneous load power, while the source supplies the average value of the load power, P_{lavg}. Therefore, average load power is given as following:

$$v_{sa}i_{sa} + v_{sb}i_{sb} + v_{sc}i_{sc} = P_{lavg}. \tag{2.25}$$

Since the harmonic component in the load does not require any real power, the source only supplies the real power required by the load. The average load power can be calculated by the moving average filter. Now combining the equations (2.19), (2.24)

and (2.25), we get the reference source currents

$$\begin{bmatrix} i_{sa}^* \\ i_{sb}^* \\ i_{sc}^* \end{bmatrix} = M^{-1} \begin{bmatrix} 0 \\ 0 \\ P_{lavg} \end{bmatrix} \tag{2.26}$$

where

$$M = \begin{bmatrix} 1 & 1 & 1 \\ (v_{sb} - v_{sc} - 3\gamma(v_{sa} - v_0)) & (v_{sc} - v_{sa} - 3\gamma(v_{sb} - v_0)) & (v_{sa} - v_{sb} - 3\gamma(v_{sc} - v_0)) \\ v_{sa} & v_{sb} & v_{sc} \end{bmatrix}$$

The reference compensator currents are given as

$$\begin{aligned} i_{fa}^* &= i_{la} - i_{sa}^* = i_{la} - \frac{(v_{sa} - v_0) + \gamma(v_{sb} - v_{sc})}{\Delta_1}(P_{lavg}) \\ i_{fb}^* &= i_{lb} - i_{sb}^* = i_{lb} - \frac{(v_{sb} - v_0) + \gamma(v_{sc} - v_{sa})}{\Delta_1}(P_{lavg}) \\ i_{fc}^* &= i_{lc} - i_{sc}^* = i_{lc} - \frac{(v_{sc} - v_0) + \gamma(v_{sa} - v_{sb})}{\Delta_1}(P_{lavg}) \end{aligned} \tag{2.27}$$

where

$$\Delta_1 = \left[\sum_{j=a,b,c} v_{sj}^2\right] - 3v_0^2,\ v_0 = \frac{1}{3}\sum_{k=a,b,c} v_{sk},\ \gamma = \tan\ \varphi^+/\sqrt{3}$$

The average power supplied by the source according to the above equation will be equal to the average power required by the load. Apart from the load average power, the source has to supply VSI losses also. When the inverter power loss P_{loss} is also incorporated in (2.27), the modified reference currents of the compensator become

$$\begin{aligned} i_{fa}^* &= i_{la} - i_{sa}^* = i_{la} - \frac{(v_{sa} - v_0) + \gamma(v_{sb} - v_{sc})}{\Delta_1}(P_{lavg} + P_{loss}) \\ i_{fb}^* &= i_{lb} - i_{sb}^* = i_{lb} - \frac{(v_{sb} - v_0) + \gamma(v_{sc} - v_{sa})}{\Delta_1}(P_{lavg} + P_{loss}) \\ i_{fc}^* &= i_{lc} - i_{sc}^* = i_{lc} - \frac{(v_{sc} - v_0) + \gamma(v_{sa} - v_{sb})}{\Delta_1}(P_{lavg} + P_{loss}). \end{aligned} \tag{2.28}$$

The term P_{lavg} is obtained using simple moving average filter over a half cycle as the oscillating part of the real power has frequency which is double the system frequency and P_{loss} is obtained from the PI controller. The error between DC voltage reference and

actual DC voltage are processed through PI controller to obtain P_{loss}. This will control the DC link voltage by adjusting the small amount of real power absorbed by the shunt inverter. This small amount of real power is adjusted by changing the amplitude of the fundamental component of the reference current. The AC source provides some active current to recharge the DC capacitor. Thus, in addition to reactive and harmonic components, the reference current of the shunt active filter has to contain some amount of active current as compensating current. This active compensating current flowing through the shunt active filter regulates the DC capacitor voltage [19].

Out of various time based theories, instantaneous symmetrical component theory with extraction of fundamental positive sequence components is simple in formulation and devoid of ambiguity over the definition of various power terms. Even though the time domain methods are faster, they are found to have certain disadvantages. So, in this project, one of the frequency based methods, Wavelet Transform, is used in order to address the power quality issues. The next section deals with the limitations of time based methods and advantages of using Wavelet Transform in the area of power quality.

2.4 Advantages of Wavelet Analysis in Power Quality

In the area of power quality, several studies have been carried out to detect and locate disturbances like lightning transients, transformer inrush currents, motor starting currents, capacitor and line-switching transients and harmonics. Analysis and understanding of transients associated with such abnormal conditions have always helped rectify the cause of the condition. The increasing complexity of power systems makes power engineers to look for improved alternative methods of transient analysis, for the purposes of designing new equipment to efficiently deal with the abnormal transient phenomena.

The present methods of analysis have limitations. For instance, performance of the time based methods such as instantaneous power theory and synchronous reference frame theory is degraded when the power quality disturbances are not the same in all phases, which is always the case in power system. The frequency domain methods such as Fourier series based analysis requires periodicity of all the time functions involved. The frequency information of a signal calculated by the classical Fourier transform is

an average over the entire time duration of the signal. If there is a local transient over some small interval of time in the signal, the transient will contribute to the FT, but its location on the time axis will be lost. Traditional Fourier analysis does not consider frequencies that evolve with time, i.e. non-stationary signals [32]. In addition, Fourier techniques suffer from some aggravating anomalies such as Gibbs' phenomena and aliasing when used for non-stationary signals. Short Term Fourier Transform (STFT) was proposed to overcome the foregoing problems to a certain extent. However, the drawback is that the window width of STFT has to be fixed prior to the analysis; this effectively means that it does not provide the required good resolution in both time and frequency, which is an important characteristic for analyzing transient signals. In addition, wavelet-based techniques are less sensitive to power system frequency oscillation since WT based methods can extract a band of frequency. In contrast, time based amplitude and phase-angle estimation algorithms must be synchronized with frequency variation using other frequency estimation algorithms [31], which are not as fast and simple as WT based algorithms in harmonic conditions. Therefore, they are more time consuming and complicated in harmonic conditions

These methods, which are based on either time or frequency domain, are not sufficient for accurate detection and characterization of power quality events when the signal is non-stationary. Wavelet Transform based methods have been proposed to overcome these drawbacks. DWT based signal processing is used in [33] to estimate harmonics and voltage sags. Though CWT provides good time resolution and good time resolution at low frequency, DWT is used in this project since CWT is redundant and computational burden is very high. Section 3.4 discusses the application of wavelet based analysis on power quality.

2.5 Summary

In this chapter,various power quality issues, DSTSTCOM structure and design of parameters and various control strategies for DSTATCOM have been explained in detail. Out of various time based control techniques, instantaneous symmetrical component theory is found to be simple in formulation and devoid of ambiguity over the definition of various power terms. Even though time based methods are faster, their performance

is degraded when the power quality disturbances are not same in all phases. In addition, time based methods are not able to compensate the source currents when the frequency of the system changes. So, due to these limitations of times based methods, Wavelet Transform is adopted in this project to address power quality issues.

CHAPTER 3

INTRODUCTION TO WAVELET ANALYSIS

With the advancement in measurement technology, an increasing volume of data is being gathered and it needs to be processed. Signal processing is generally called upon when there is a need to extract specific information from the raw data. Different techniques have been used for the identification, classification and characterization of the raw data. The techniques used vary, depending on the characteristics of the phenomena. Wavelet analysis is a technique for decomposing a function or data into multiple components corresponding to different frequency bands. This allows one to study each component separately. The main idea existed since the early 1800s when Joseph Fourier first discovered that signals could be represented as superposed sine and cosine waves, forming the basis for the infamous Fourier analysis. From the beginning of 1990s, it began to be utilized in science and engineering, and has been known to be particularly useful for analyzing signals that can be described as aperiodic, noisy, intermittent, or transient [25]. With these attributes, it is widely used in many applications including data compression, earthquake prediction, and mathematical applications such as computing numerical solutions for partial differential equations [26]. Wavelet theory provides a unified framework for a number of techniques which had been developed independently for various signal processing applications. In particular Wavelet Transform (WT) is of interest for the analysis of non-stationary signals.

For some applications, it is desirable to see the WT as a signal decomposition onto a set of basis functions called $waveletes$. They are obtained from a single prototype wavelet by dilation and contractions (scaling) as well as shifts. In a WT domain, the notion of $scale$ is introduced as an alternative to frequency. This means that a signal is mapped into a time-scale plane.

There are several types of wavelet transforms and preference is done depending upon the application. For a continuous input signal, the time and scale parameters can be continuous leading to the Continuous Wavelet Transform (CWT). The WT can be defined for discrete time signals leading to a Discrete Wavelet Transform (DWT).

3.1 Continuous Wavelet Transform

The CWT of a signal $f(t)$ is defined as

$$F(a,\tau) = \frac{1}{\sqrt{a}} \int f(t)\psi^*(\frac{t-T}{a})dt \tag{3.1}$$

where a is the scale of the transforming wavelet along the frequency axis and τ is the translation of the transforming wavelet along the time axis. Physically, the integral in (3.1) can be understood as the signal $f(t)$ being filtered through a series wavelet mother functions translated by τ and dilated by a. A contracted version of the mother wavelet would correspond to high frequency and is obtained for the scale $a > 1$. In order to obtain the low-frequency information necessary for full representation of the original signal $s(t)$, it is necessary to find the wavelet coefficients for scale $a > 1$. This is achieved by introducing a scaling function $\phi(t)$ which is an aggregation of the mother wavelets $\psi(t)$ at scales greater than 1. A function $\psi(t)$ would be considered as a mother wavelet if $\psi \in \mathrm{L}^2(R)$ and with mean zero, ie.,

$$\int_{-\infty}^{+\infty} \psi(t)dt = 0. \tag{3.2}$$

Some of the commonly used mother wavelets are given below.

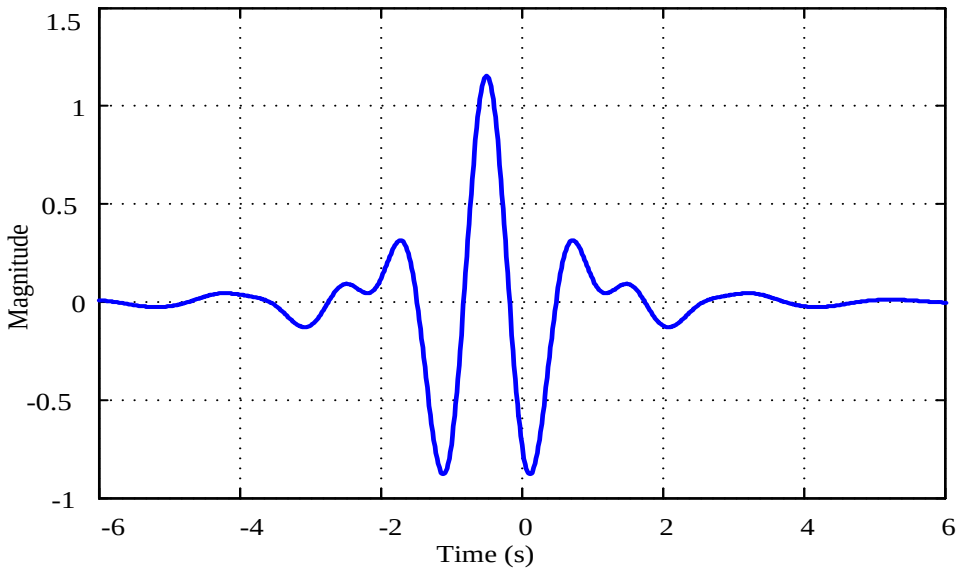

Figure 3.1: Meyer wavelet

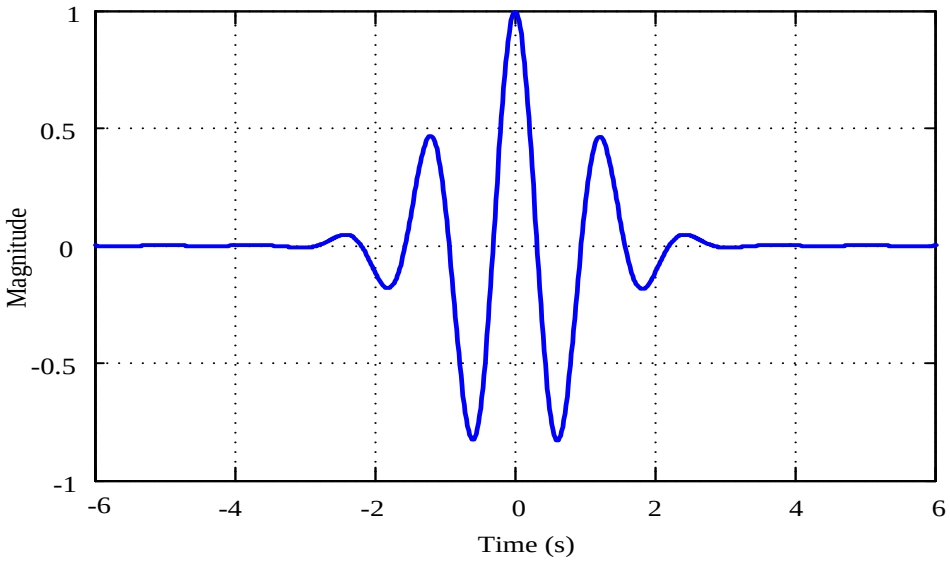

Figure 3.2: Morlet wavelet

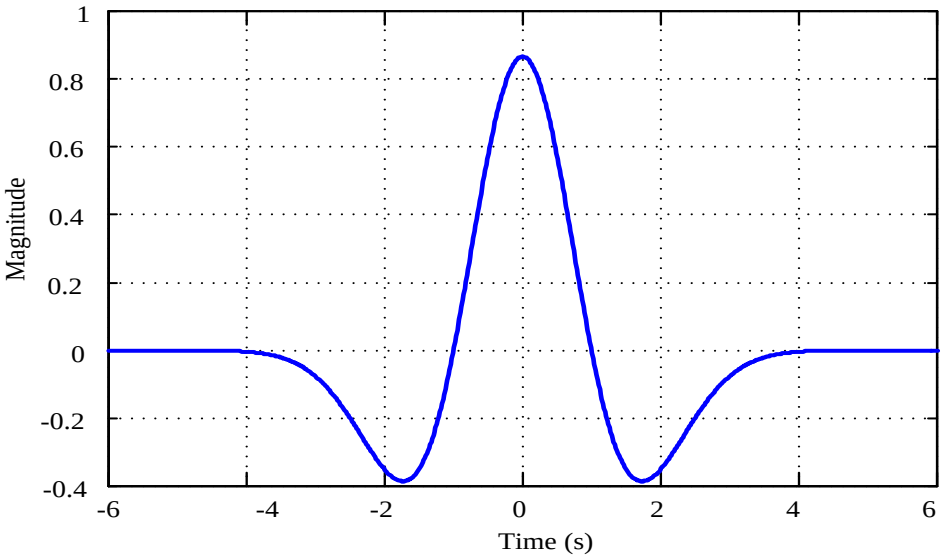

Figure 3.3: Mexican hat wavelet

The translated and scaled versions of $\psi(t)$ by factors u and s respectively, in normalized form, are obtained from the expression

$$\psi_{u,s}(t) = \frac{1}{\sqrt{s}}\psi\left(\frac{t-u}{s}\right)dt. \tag{3.3}$$

Any function $f(t) \in \mathrm{L}^2(R)$ can be represented as

$$f(t) = \frac{1}{\mathrm{C}_\psi}\int_0^{+\infty}\int_{-\infty}^{+\infty}\mathrm{W}f(u,s)\frac{1}{\sqrt{s}}\psi\left(\frac{t-u}{s}\right)du\frac{ds}{s^2} \tag{3.4}$$

where $\hat{\psi}(w)$ indicates the admissibility condition and $\mathrm{W}f(u,s)$ is the wavelet transform of $f(t)$ at time u and scale s. These are given as follows;

$$\mathrm{C}\psi = \int_0^{+\infty} \frac{|\hat{\psi}(w)|^2}{\omega} d\omega < +\infty \tag{3.5}$$

where, $\hat{\psi}(w)$ is the Fourier transform of $\psi(t)$ given by

$$\hat{\psi}(w) = \int_{-\infty}^{\infty} \psi(t) e^{-i\omega t} dt \tag{3.6}$$

The continuous wavelet transform of $f(t)$ with the wavelet function ψ is

$$\mathrm{W}f(u,s) = \frac{1}{\sqrt{s}} \int_{-\infty}^{\infty} f(t) \psi^*(\frac{t-u}{s}) dt \tag{3.7}$$

where, $\hat{\psi}(w)$ is the complex conjugate of ψ. Though CWT based signal analysis has several advantages, it's drawback is the requirement of high computational cost for real time implementation.

3.2 Discrete Wavelet Transform

Discrete Wavelet Transform (DWT) of a signal $f(t)$ is obtained if we incorporate binary dilations (2^j) and dyadic translations ($k/2^j$) in the wavelet function, ψ, where j and k are integers. The DWT is based on the following equation.

$$DWT[m,k] = \frac{1}{\sqrt{a_0^j}} \sum_{n=0}^{N-1} f[n] \psi \left(\frac{k - n a_0^j}{a_0^j} \right) \tag{3.8}$$

where $\psi(n)$ is the mother wavelet of which there is an infinite number of possible wavelets that can be used. Some of the discrete mother wavelets are given in Fig. 3.4.

The signal analyzed $f(t)$ is sampled and passed through a high pass filter $\bar{g}$ and a low pass filter $\bar{h}$ and then down sampled by two to give detail and approximation co-efficients respectively. This process is repeated to get finer details and coarse approximation of the signal. This is called Multi Resolution Analysis (MRA) [27].

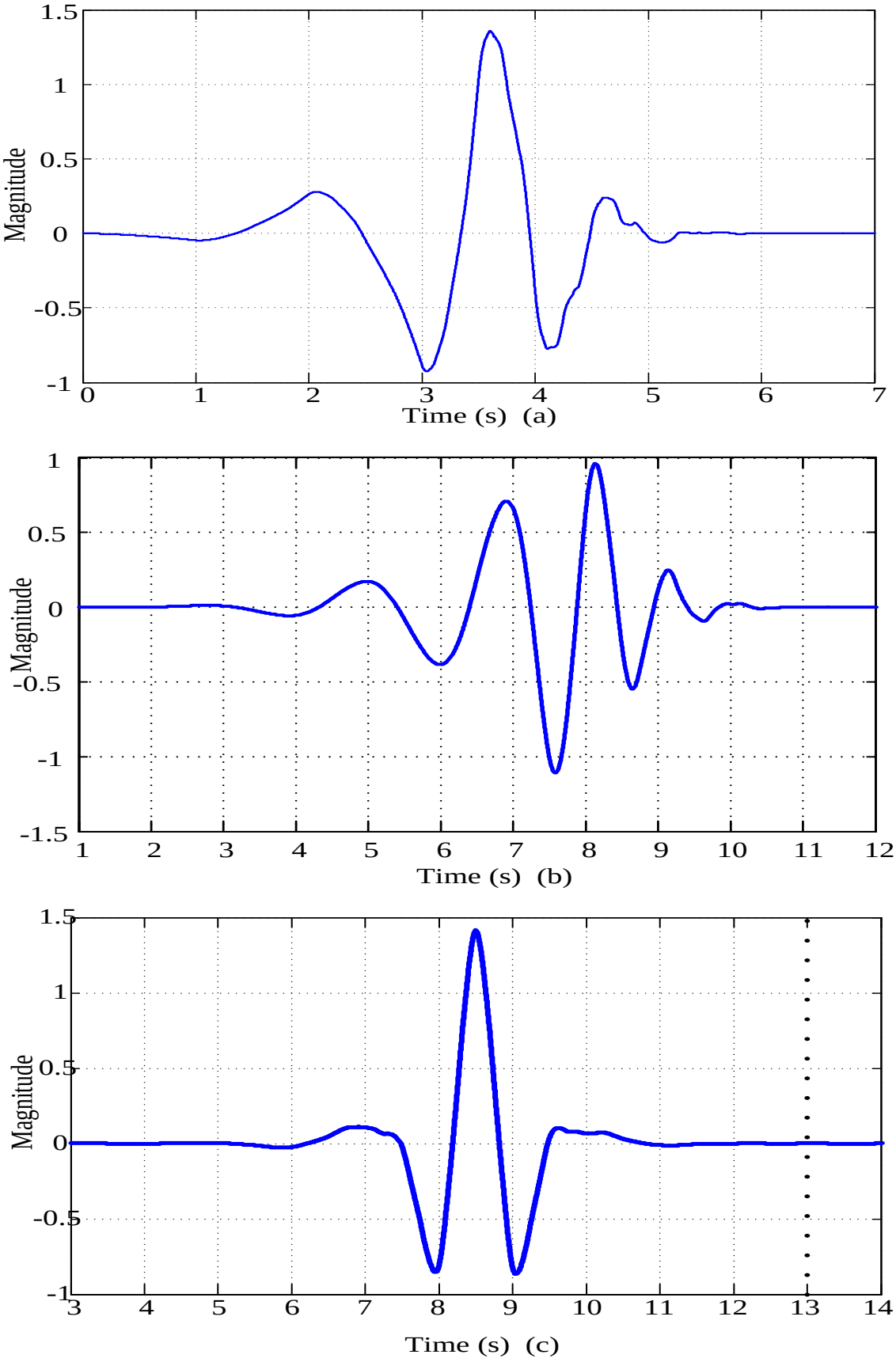

Figure 3.4: Wavelet functions of (a) Daubechies 4 wavelet (b) Daubechies 8 wavelet (c) Coiflet wavelet

Table 3.1: Comparison of computational cost of various methods

Method	Computational cost
DFT	$O(N \times N)$
FFT	$O(N \log_2 N)$
CWT	$O(N \times N)$
CS-CWT	$O(d \times N)$
Biorthogonal DWT	$O(N)$

Wavelet transform is used in many applications including signal suppression, denoising etc. In addition,the localization property of wavelet enables discontinuities or breakdown points to be easily identified. It is therefore widely applied for detection of the onset of certain events and to detect the exact instant of the occurrence. Instead of the highly redundant CWT, DWT is often used as it is more efficient computationally and requires less memory storage. Unlike CWT where the expansion is performed on any arbitrary scale, DWT follows a certain discrete expansion pattern determined by the selection of a factor a_0. The most widely used pattern is called dyadic expansion with $a_0 = 2$. Successful application of wavelet transform depends heavily on the mother wavelet. The next section describes the procedures to be followed for the selection of mother wavelet.

3.3 Selection of Mother Wavelet

Generally, the objective of the wavelet analysis and the characteristic of the analyzed object decide the mother wavelet. For power quality applications, it has been quoted to preferably be oscillatory, with a short support and has at least one vanishing moment [28]. The oscillatory feature is trivial as power networks are AC and many phenomena including transients are oscillatory in nature. Vanishing moments is a useful quality to have since it helps to suppress regular part of the signal, highlighting the sharp transitions [29]. If a fast algorithm is needed, the wavelet must be achievable via FIR filters. If the approximation part of the analysis is needed, scaling function becomes necessary. If reconstruction is needed, biorthogonal wavelets have some advantages compared to orthogonal wavelets. The symmetry and exact reconstruction are both possible with biorthogonal wavelet functions. These wavelets can be defined through two scaling filters for reconstruction and decomposition, respectively [30]. For this project, Biorthog-

onal 5.5 wavelet is chosen because of aforementioned reasons.

3.4 Wavelet Applications in Power Quality

The ability of wavelet transform in decomposing a signal into multiple frequency bands with optimized resolutions makes it an attractive technique for analyzing power quality waveform. WT is particularly used to study disturbance transient waveform, where it is necessary to examine different frequency components separately. This section deals with several popular uses of wavelet transform in the analysis of power quality disturbances.

3.4.1 Detection of PQ Events

The time and space localization property of wavelet transform makes it highly suitable for analysis of power system transients, happening due to load turning-on and faults [39]. Fig. 3.5 and Fig. 3.6 show a voltage sag waveform and capacitor switching transient decomposed into several levels with different frequency bands respectively. In each levels several distinct short bursts are observed in both the waveforms which can be used as a discriminating feature between the events.

Table 3.2: Frequency band in DWT

Wavelet Co-efficients	Frequency Range (Hz)
D_1	600 - 1200
D_2	300 - 600
D_3	150 - 300
D_4	75 - 150
D_5	37.5 - 75

Fig. 3.5(a) shows a voltage sag at $t = 0.1s$ with 5 cycles duration and the corresponding characterization using wavelet method. This signal is sampled at 2400 Hz and decomposed using MRA up to 5 levels. The corresponding frequency information

is given in Table 3.2. Fig. 3.5(b) is the level 1 (D_1) of MRA which corresponds to 600 Hz to 1200 Hz where small bursts are observed during voltage sag. Fig. 3.5(c) and Fig. 3.5(d) correspond to level 2 (D_2) and level 3 (D_3) of MRA respectively, in which the change during voltage sag is clearly visible. Fig. 3.5(e) (D_4) is level 4 of MRA which corresponds to 75 Hz to 150 Hz. Level 5 of MRA is shown in Fig. 3.5(f) which corresponds to the fundamental component of the voltage signal.

Fig. 3.6(a) shows the capacitor switching transient occurring at $t = 0.1s$. Fig. 3.6(b) shows the Level 1 of MRA which corresponds to 600 Hz to 1200 Hz. High frequency peaks indicate sharp changes in the signal. These peaks are used to detect changes in signal disturbances. Fig. 3.6(c) and Fig. 3.6(d) correspond to level 2 (D_2) and level 3 (D_3) of MRA respectively, in which the change during capacitor switching transient is clearly visible.Fig. 3.6(e) is level 4 of MRA and Fig. 3.6(f) gives the fundamental component of the voltage during transient.

In order to detect a voltage sag or a transient, each peak detected in the high frequency band is compared with a normal value. Therefore, a part of the signal is assumed to be disturbance-free, and is taken as reference and leads to 50, 300 and 600 Hz standard values. The next part of the signal is analyzed. Each peak exceeding these standard values is considered as a major signal discontinuity and the corresponding part is observed. Moreover, a distinction is made between the peaks. Duration and the number of peaks exceeding standard values differentiate transient events from voltage sags. Sharp and short peaks correspond to simple voltage sags or surges, whereas long peak corresponds to high frequency transients [34].

3.4.2 Characterization of PQ Events

As an indication of severity of short duration voltage variations like voltage sag, swell etc, magnitude and duration of variation are considered. Traditionally, RMS computation is used to derive the magnitude while the duration is taken as the time period the RMS magnitude stays below/above certain threshold for swells. RMS method is generally considered as sufficient, but the wavelet approach has been shown to have produced more accurate results that would be useful for determining the causes of such variations.

In the case of voltage sags, aggregated high frequency data from Level 1 and Level 2 (600 Hz and 300 Hz) are combined with 50 Hz data to reconstruct the shape of the voltage sag [35]. Each high frequency peak indicates an unusual event. At this instant, the magnitude of voltage is measured on the 50 Hz profile. Data from the various frequency profiles can be combined and duration of the event can be found out by measuring distance between the peaks. It can be shown that this approach works well too for very short voltage variation with duration less than half a cycle.

3.4.3 Classification of Power Quality Events

Each levels of wavelet coefficients over different scales can be thought as uneven distribution of energy across the multiple frequency bands. This distribution of energy forms patterns that can be used to classify between different power quality events. If the selected wavelet and scaling functions form an orthonormal set of basis, then the Parseval theorem can be used to relate energy of the signal to the values of the coefficients. This means that the norm or energy of the signal can be separated according to the following multiresolution expansion:

$$\sum_{a} |f[n]|^2 = \sum_{k} |s_{j_0(k)}|^2 + \sum_{j \geq j_0}^{N-1} \sum_{k=1} |w_{j(k)}|^2 \tag{3.9}$$

These squared wavelet coefficients are shown to be useful features for identifying power quality events. Statistics of these values can be used to identify transformer energization, converter operation, capacitor energizing and restriking. The maximum value of the squared coefficients in each scale or its average is found to be different before, during, and after the occurrence of these events. Changes in these values are used as the feature for its identification [36].

3.4.4 Reference Quantity Generation for Custom Power Devices

Developing control strategies for the reference quantity generation for custom power devices has been a great challenge for power system engineers. Various time based methods and their limitations have been discussed in Section 2.2. In order to achieve the compensation of current harmonics, reactive power and unbalance with a better

performance, Real Discrete Wavelet Transform (RDWT) with biorthogonal wavelet is proposed in this project.

3.5 Summary

Wavelet transform is quickly becoming the choice method for processing power quality data. This is due to its excellent time and frequency localization capability, and the flexibility in implementation. But more flexibilty comes with a cost of more decisions to be made. Selection of mother wavelet, using CWT or DWT and the number of decomposition levels are the three major challenging decisions that can affect the performance of the whole system significantly. In this chapter, WT is shown to be effective for characterizing and classifying switching transients and short-duration voltage variations.

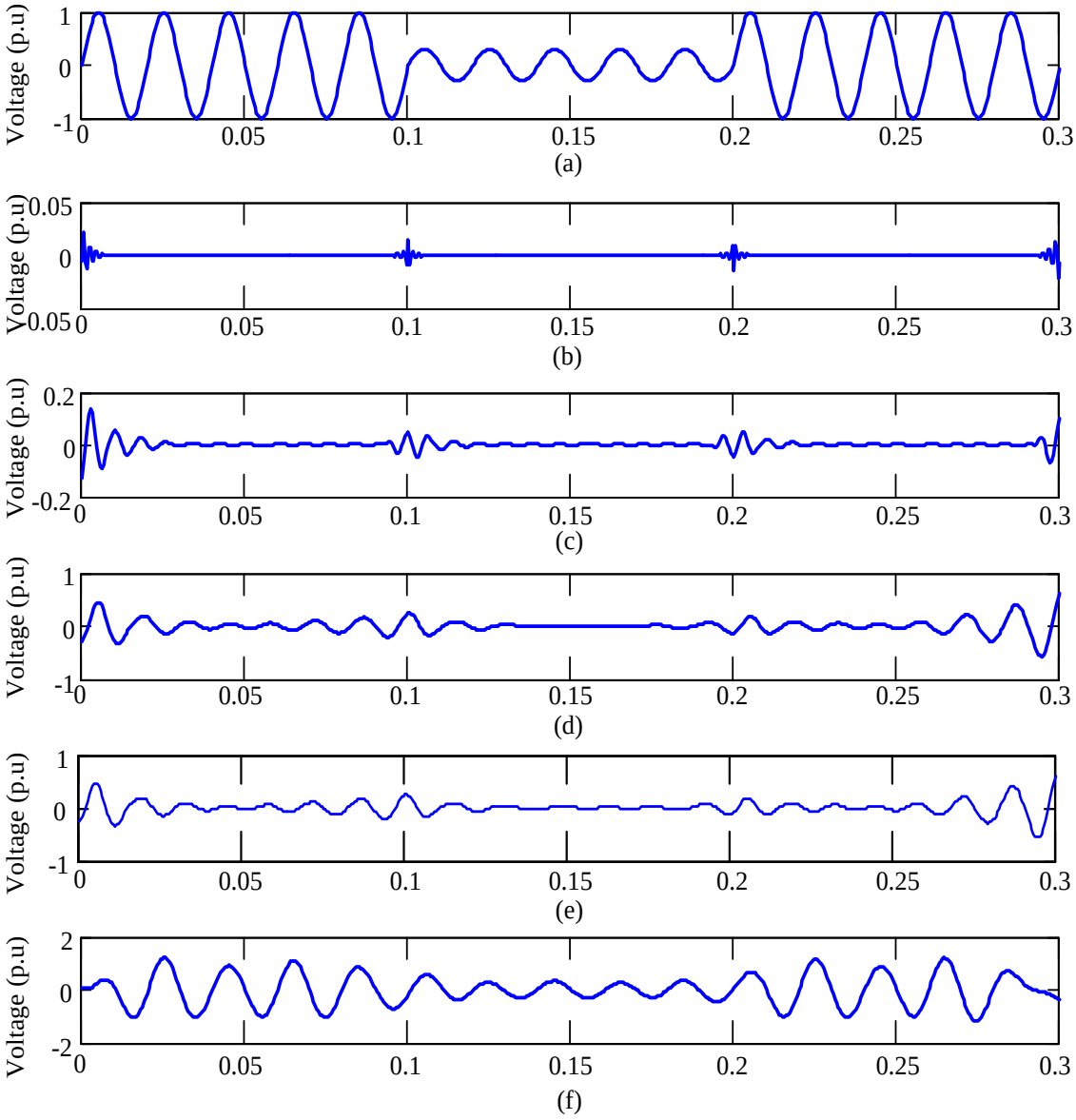

Figure 3.5: Simulation results during voltage sag at $t = 0.1s$ to $t = 0.2s$ (a) Voltage (b) Level 1 of MRA (c) Level 2 of MRA (d) Level 3 of MRA (e) Level 4 of MRA (f) Level 5 of MRA which corresponds to the fundamental component.

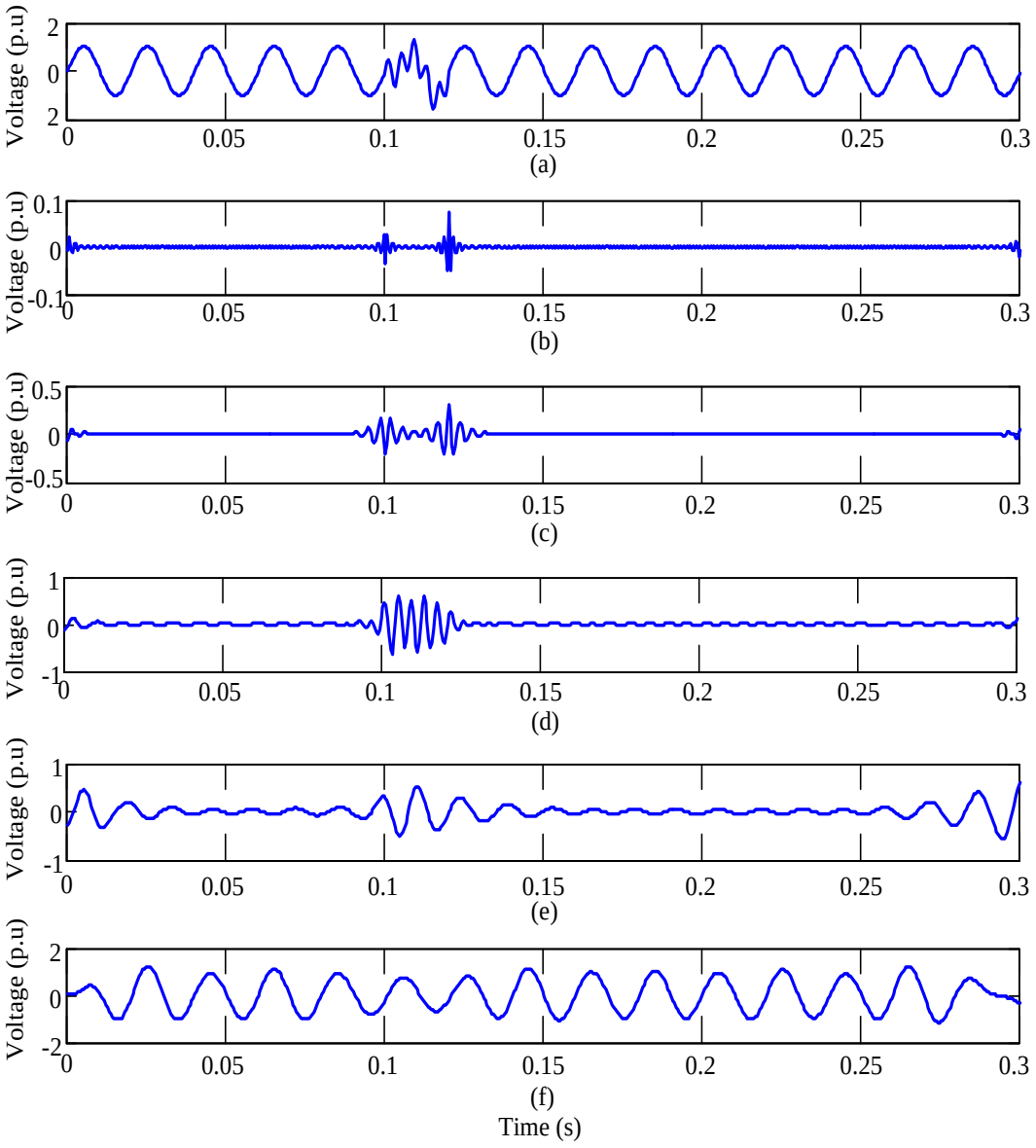

Figure 3.6: Simulation results during capacitor switching transient (a) Voltage (b) Level 1 of MRA (c) Level 2 of MRA (d) Level 3 of MRA (e) Level 4 of MRA (f) Level 5 of MRA which corresponds to the fundamental component.

CHAPTER 4

PROPOSED REFERENCE QUANTITY ESTIMATION FOR DSTATCOM

In recent years, shunt active power filters (SAPFs) have been widely investigated for the compensation of harmonics, unbalance, and reactive components of the load current i_L. A big attempt is made to improve the performance of DSTATCOM by introducing a comprehensive control strategy to compensate for various distortions of the load currents. However, drawbacks of the existing methods make them ineffective in some conditions.

Many of these control strategies, such as instantaneous reactive power theory, synchronous reference frame (SRF) theory, and Instantaneous symmetrical component theory assume that the distortion of load currents and source voltages are equal in three phases. However, in practical systems, this is an incorrect assumption. Moreover, available control strategies estimate changes in amplitude of load current at least one cycle after the beginning time of the change. Therefore, the speed of the DSTATCOM compensation decreases noticeably and resulting in increased switching power losses and dc-link voltage oscillation, and the compensator operation may become unstable. Furthermore, if the power system frequency deviates from its nominal value, the control system of DSTATCOM must be synchronized with frequency variations. However, most of the well known algorithms cannot quickly estimate frequency variations in the presence of harmonics.

A comprehensive control strategy for DSTATCOM should be simple, accurate, and should be able to extract most of the voltage and current distortions accurately even under the power system frequency variation. This project proposes a novel estimation technique and a new control strategy for the DSTATCOM system. The proposed estimation technique is based on Discrete Wavelet Transform (DWT) and Multi-Resolution Analysis (MRA) to extract the fundamental component amplitude and phase angle of load currents and source voltages. The proposed control strategy is capable of extracting most of the load current and source voltage distortions successfully.

Table 4.1: Frequency band in DWT

Wavelet Co-efficients	Frequency Range (Hz)
D_1	32000 - 64000
D_2	16000 - 32000
D_3	8000 - 16000
D_4	4000 - 8000
D_5	2000 - 4000
D_6	1000 - 2000
D_7	500 - 1000
D_8	250 - 500
D_9	125 - 250
D_{10}	62.5 - 125
A_{10}	0 - 62.5

4.1 Estimation of Fundamental Component

Wavelets have been successfully applied for signal analysis. The signal to be analyzed is sampled at 128 kHz and is subjected to MRA as discussed in Section 3.2 using discrete bi orthogonal 5.5 wavelet as mother wavelet. This is depicted in Fig. 4.1. The signals are described by these wavelet coefficients as given below.

$$i(t) = \sum_{k=0}^{2^{j_0-1}} c_{j_0,k}\phi_{j_0,k}(t) + \sum_{j\geq j_0}^{N-1}\sum_{k=0}^{2^{j-1}} d_{j,k}\psi_{j,k}(t) \tag{4.1}$$

$$\text{with } c_{j_0,k} = \langle i(t), \phi_{j_0,k}(t)\rangle \text{and } d_{j,k} = \langle i(t), \psi_{j,k}(t)\rangle$$

where j and k are the wavelet frequency scale and wavelet time scale, respectively,c and d are the wavelet coefficients and $\langle , \rangle$ is the inner product operation. $\psi(t)$ and $\phi(t)$ are the mother and scaling functions, respectively. Low pass and high pass filters for the decomposition and reconstruction of the bi orthogonal 5.5 wavelet are given in Fig. 4.2. The signal decomposition up to ten levels yield the frequency information as given in Table 4.1, where D_1 to D_{10} are detail co-efficients and A_{10} is the approximation co-efficient. The fundamental component can be obtained by passing A_{10}, which contain all frequency components between 0 - 62.5 Hz, through low-pass reconstruction filter. Fig. 4.3(a) shows a distorted current waveform and Fig. 4.3(b) shows the extracted fundamental using bi-orthogonal 5.5 DWT.

The computational complexity of DWT is $O(N)$ operations for a signal of size N which is lesser than that of Morlet CWT for which it is $O(N \times N)$ [37]. CWT is

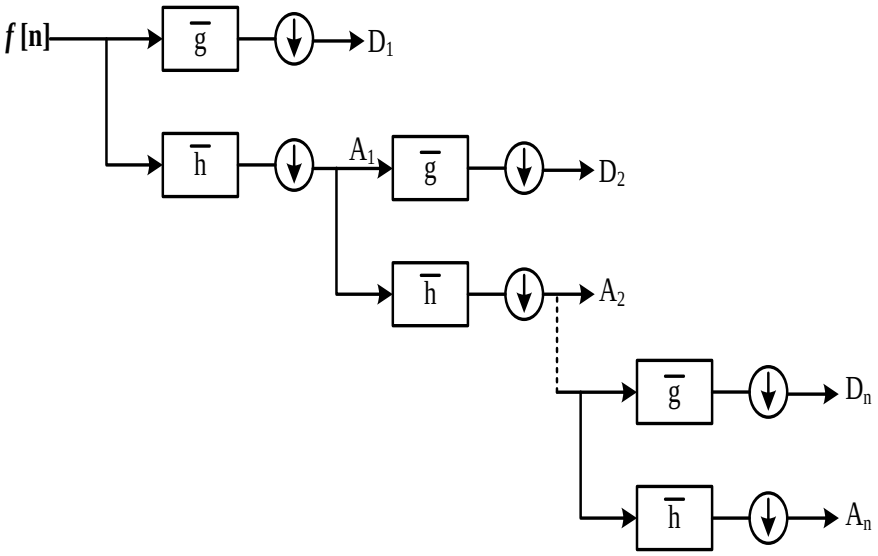

Figure 4.1: Multi resolution analysis

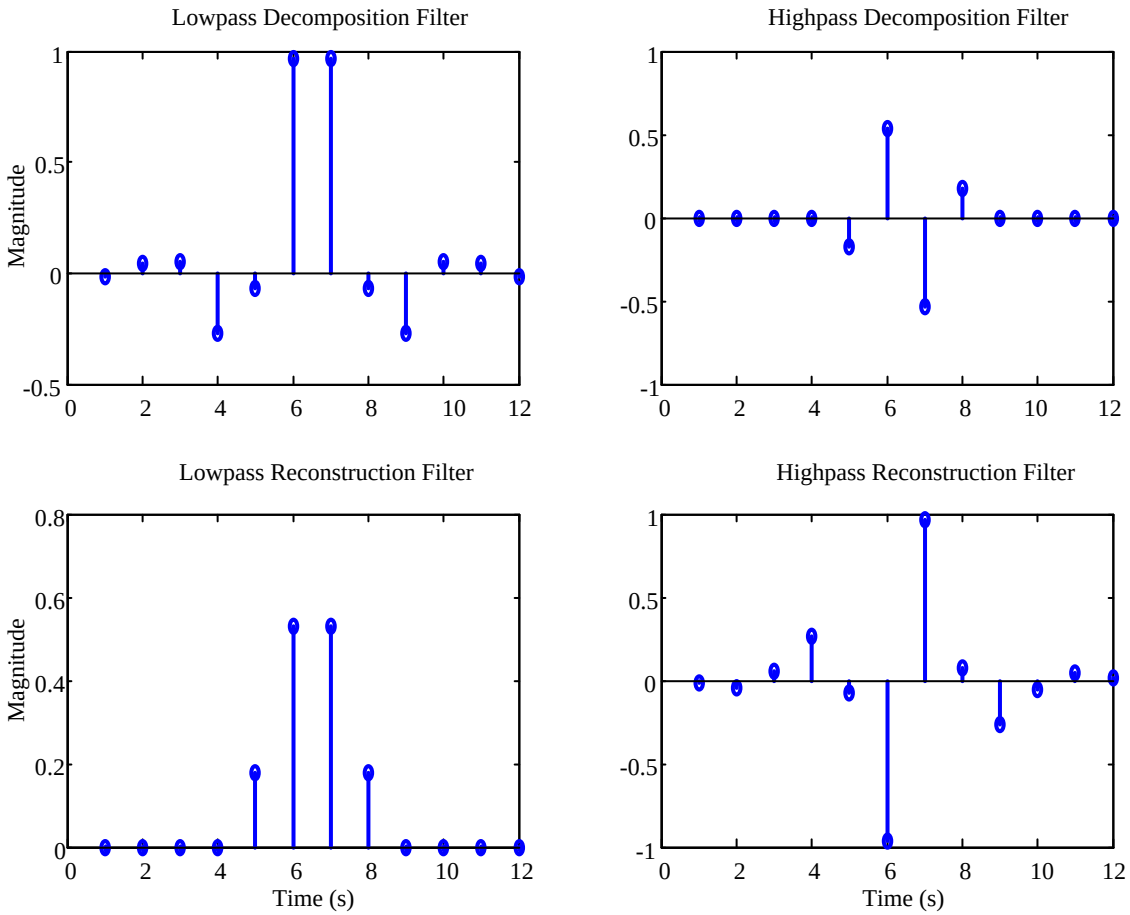

Figure 4.2: Filters for the discrete bi-orthogonal 5.5 wavelet

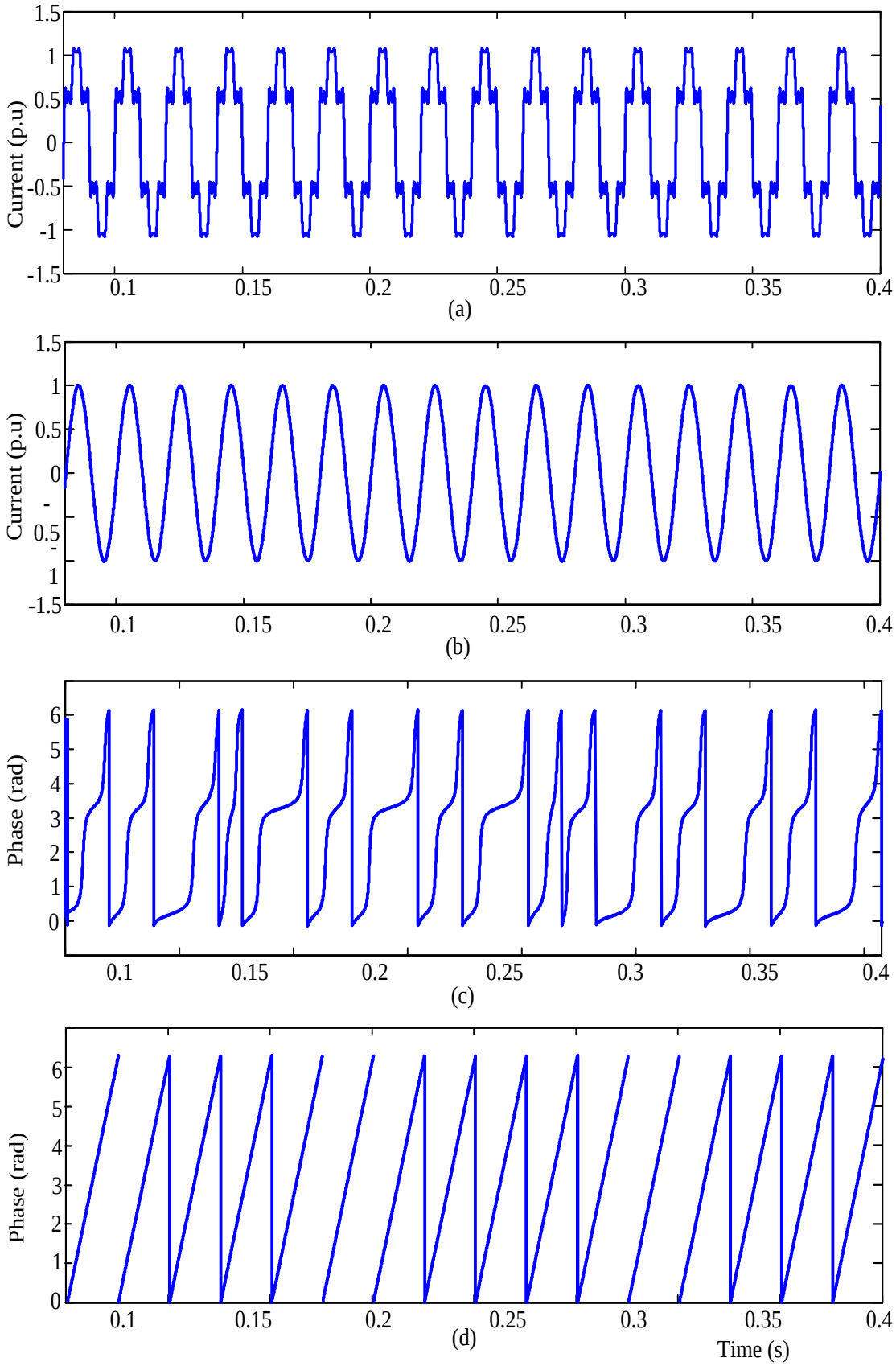

Figure 4.3: Fundamental Extraction using bi-orthogonal 5.5 DWT (a) Sampled distorted current waveform (b) Extracted fundamental using Bi-orthogonal 5.5 DWT (c) Extracted phase information using Morlet CWT (d) Extracted phase information using Bi-orthogonal 5.5 DWT.

preferred for the reference quantity generation in custom power devices since DWT is considered to have lack of phase information even though CWT is redundant and computational burden is much higher than DWT. This project proposes a novel method to extract the fundamental component using Bi-orthogonal DWT which is non-redundant, simpler, faster and requires less computational cost.

4.2 Phase Extraction Method Using DWT

All popular WT-based phase extraction methods utilize complex WT (CWT), since the argument of complex coefficients of CWT is related to the phase angle of the analyzed signal. The most commonly used CWT is Complex Continuous WT (CCWT). The commonly used continuous complex wavelets are Morlet wavelet [38] and complex Gaussian wavelets. Besides continuous complex wavelets, discrete complex wavelets such as complex Daubechies wavelets and other complex orthogonal or biorthogonal wavelets are also applied in some cases. In contrast to Real Discrete WT (RDWT), complex discrete WT (CDWT) with these complex discrete wavelets will take double computing time when associated filters of real and complex wavelets are with the same length.

This project focuses on obtaining phase information by using DWT. Theoretically, the DWT-based phase information extraction method is possible since orthonormal and biorthogonal DWTs are loss-less ones which means that all information of the analyzed signal is conserved in wavelet coefficients of the DWTs. Instead of extracting phase information directly from wavelet coefficients as done in CWT-based methods, wavelet coefficients are made phase quadrature then pick up phase information from the phase-quadrature coefficients. This approach not only can extract phase information but also can inherit all merits of DWT [40].

Suppose f_s is the sampling frequency of the analyzed discrete signal $x(n)$ and $T_s = 1/f_s$ is the sampling interval. In terms of z-transform, the variable z on unit circle is

$$z = \exp(-i\omega T_s) = e^{-i\Delta\varphi(\omega)} = \exp(-i2\pi f/f_s) = e^{-i2\pi/N} \tag{4.2}$$

where $\Delta\varphi(w) = wT_s$ and $N = f_s/f$. After implementing DWT of $x(n)$, the resulting

real approximate component $s(n)$ and its z-transform $S(z)$ are

$$\begin{aligned} s(n) &= \sum h(l-n)x(l) \\ &= \sum h(k)x(k+n) \qquad k = k_{g\min} - k_{g\max} \\ S(z) &= H^*(z)X(z) \end{aligned}$$

where $H(z)$ is the low-pass filter associated with the Bi-orthogonal 5.5 wavelet and H^* is its complex conjugate. Let $s(n)$ be the approximate component of Bi-orthogonal DWT, suppose

$$s_e(n) = (s(n) + s(n-1))/2 \tag{4.3}$$

$$s_o(n) = (s(n) - s(n-1))/2 \tag{4.4}$$

Suppose z-transforms of $s_e(n)$ and $s_o(n)$ be $S_e(z)$ and $S_o(z)$, respectively. Then,

$$\begin{aligned} S_e(z) &= \frac{S(z) + z^{-1}S(z)}{2} \\ &= e^{i\Delta\varphi/2}\,\frac{e^{-i\Delta\varphi/2} + e^{i\Delta\varphi/2}}{2} S(z) \\ &= cos(\Delta\varphi/2)\; e^{i\Delta\varphi/2} H^*(z)\; X(z) \\ &= H_e^*(z)\; X(z) \end{aligned} \tag{4.5}$$

$$\begin{aligned} S_o(z) &= \frac{S(z) - z^{-1}S(z)}{2} \\ &= e^{i\Delta\varphi/2}\,\frac{e^{-i\Delta\varphi/2} - e^{i\Delta\varphi/2}}{2} S(z) \\ &= -i * sin(\Delta\varphi/2)\; e^{i\Delta\varphi/2} H^*(z)\; X(z) \\ &= e^{-i\pi/2}\; H_o^*(z)\; X(z) \end{aligned} \tag{4.6}$$

where

$$\begin{aligned} H_e^*(z) &= cos(\Delta\varphi/2)\; e^{i\Delta\varphi/2} H^*(z) \\ H_o^*(z) &= sin(\Delta\varphi/2)\; e^{i\Delta\varphi/2} H^*(z) \end{aligned}$$

From the shift theorem of the z-transform, the real factors $cos(\Delta\varphi/2)$ in 4.5 and $sin(\Delta\varphi/2)$ in 4.6 influence the amplitudes of $S_e(z)$ and $S_o(z)$, respectively, but not their phases, whereas the complex factors $e^{i\Delta\varphi/2}$ and $e^{-i\pi/2}$ influence their phases but not their amplitudes. Therefore, $S_e(z)$ and $S_o(z)$ do not have identical effects on the amplitude of $x(n)$, and $S_o(z)$ adds a $-\pi/2$ phase shift to all frequency components of $x(n)$ compared with $S_e(z)$. It has been proved that $s_e(n)$ and $s_o(n)$ are phase quadrature signals but their amplitudes are not identical. So

$$s_q(n) = s_e(n) + i * s_o(n) \tag{4.7}$$

Assume $x(n)$=$A\sin(2n\pi/T)$, so s_q can be further expressed as [41]

$$s_q(n) \quad = U_{sr}(n)\cos(2n\pi/T) + iU_{si}\sin(2n\pi/T) \tag{4.8}$$

Since magnitudes of $s_e(n)$ and $s_o(n)$ are not identical, U_{sr} and U_{si} are different. Given the ratio $P_r = U_{si}/U_{sr}$ we can create a modified detail component:

$$\begin{aligned} \tilde{s}(n) &= P_r s_e(n) + i s_o(n) \\ &= \tilde{U}_{si}(n)(\cos(2n\pi/T) + i\sin(2n\pi/T)) \\ &= \tilde{s}_e(n) + i\tilde{s}_o(n) \end{aligned} \tag{4.9}$$

where $\tilde{s}_e(n)$ = $P_r * s_e(n)$, $\tilde{s}_o(n) = s_o(n)$. Both of these quantities form a pair of quadrature signals in WT domain. Based on (4.9), since A is constant, we have,

$$\begin{aligned} P_r s_e(n))^2 + s_o(n)^2 &= (P_r s_e(n-1))^2 + (s_o(n-1))^2 \\ P_r(n) &= \sqrt{\left|\frac{(s_e(n))^2 - (s_e(n-1))^2}{(s_o(n))^2 - s_o(n-1)^2}\right|} \end{aligned} \tag{4.10}$$

With P_r, we can create complex component as

$$\tilde{s}(n) \quad = \quad P_r * s_e(n) + i * s_o(n) \tag{4.11}$$

Phase Information can be extracted from $\tilde{s}(n)$ as

$$angle(\tilde{s}(n)) = \arctan\left[\frac{P_r * s_e(n)}{s_o(n)}\right] \tag{4.12}$$

The extracted phase of the fundamental current, using complex Morlet wavelet transform and Real Discrete Wavelet Transform are shown in Fig. 4.3(c) and Fig. 4.3(d) respectively.

4.3 Positive Sequence Extraction Using DWT

According to the concept of symmetrical components, any unbalanced three-phase vectors can be decomposed into a set of balanced three-phase vectors. This set consists of positive-sequence components having the same phase sequences (abc), negative-sequence components with phase sequence (acb) and zero-sequence components having equal magnitudes with the same phase. The symmetrical components transformation matrix A can be used to transform from phase components to sequence components and its inverse A^{-1} can be used for transforming from sequence components to the original phases using the operator a.

$$A = \frac{1}{3}\begin{bmatrix} 1 & 1 & 1 \\ 1 & a^2 & a \\ 1 & a & a^2 \end{bmatrix}, A^{-1} = \begin{bmatrix} 1 & 1 & 1 \\ 1 & a & a^2 \\ 1 & a^2 & a \end{bmatrix}$$

where a is phase shift operator with $a = 1\angle 120$, and $a^2 = 1\angle -120$.

Symmetrical components theory can be defined in the time-frequency domain by applying time shift instead of phase shift for the phase voltage and current. So, a represents a time advance while the a^2 represents a time delay in the time-frequency domain. Thus samples in the time equivalent to the phase shift operator a are shifted instead of shifting the angle [42].

Following the application of the DWT, the voltage and current of any phase x can be expressed using (4.1)

$$v_x = \sum_k c'_{j_\circ,k,x}\phi_{j_\circ,k}(t) + \sum_{j\geq j_\circ}\sum_k d'_{j,k,x}\psi_{j,k}(t) \tag{4.13}$$

$$i_x = \sum_k c_{j_\circ,k,x}\phi_{j_\circ,k}(t) + \sum_{j\geq j_\circ}\sum_k d_{j,k,x}\psi_{j,k}(t) \tag{4.14}$$

Note that x can be any phase (a,b,c), while ϕ is the scaling function, ψ is the wavelet function, j_0 is the scaling level, j is the wavelet level and k is the time index. The scaling function coefficients c and the wavelet coefficients d are defined as

$$c'_{j_\circ,k,x} = \langle v_x, \phi_{j_\circ,k}\rangle, \quad c_{j_\circ,k,x} = \langle i_x, \phi_{j_\circ,k}\rangle \tag{4.15}$$

$$d'_{j,k,x} = \langle v_x, \psi_{j,k}\rangle, \quad d_{j,k,x} = \langle i_x, \psi_{j,k}\rangle \tag{4.16}$$

Time shift is applied to the voltages and currents of phases b and c in order to get the sequence components in the wavelet domain. Time advance $(k+m)$ is applied to the coefficients, where m represents the time corresponding to the angle 120°, to obtain the advanced versions of the current of phases b and c to be i'_b, and i'_c and shifted versions of the voltages of the same phases to be v'_b, and v'_c, respectively. By applying time delay $(k-m)$ to the coefficients, delayed versions of the current, i''_b and i''_c and voltage, v''_b and v''_c of phases b and c are obtained [42]. Finally, the sequence components in the wavelet domain can be obtained as follows:

$$i^0 = \frac{1}{3}[i_a + i_b + i_c], \qquad v^0 = \frac{1}{3}[v_a + v_b + v_c] \tag{4.17}$$

$$i^+ = \frac{1}{3}\left[i_a + i'_b + i''_c\right], \qquad v^+ = \frac{1}{3}\left[v_a + v'_b + v''_c\right] \tag{4.18}$$

$$i^- = \frac{1}{3}\left[i_a + i''_b + i'_c\right], \qquad v^- = \frac{1}{3}\left[v_a + v''_b + v'_c\right] \tag{4.19}$$

4.4 Control Strategy for DSTATCOM

The proposed wavelet-based estimation technique can be used for the DSTATCOM control system to derive the fundamental positive sequence of load currents and the source voltage phase, and then to obtain the reference current waveforms. The reference current waveform for DSTATCOM should be subtracted from the original distorted waveforms to extract the distortion of the load currents.

Fig. 4.4 shows the block diagram of the proposed control strategy for DSTATCOM. The fundamental component of load current i_l is extracted using the proposed wavelet-based estimation technique discussed in the previous section. For online operation of wavelet algorithm, load current is given to DWT block through a buffer. Buffer size can

be determines by

$$\text{Buffer size} = 2^j$$

where j is the predefined wavelet decomposition level to obtain desired frequency band. We can select buffer size as 2^j or multiples of 2^j. Input signal is decomposed using wavelet at specific level to get the frequency band corresponding to the fundamental. By doing MRA in 10 levels with sampling frequency 128kHz, approximate component is calculated to have the desired fundamental as given in Table 4.1. The approximate component is then reconstructed using Inverse DWT and the output is unbuffered. If the loads are unbalanced, the obtained fundamental current will have unbalances too. The positive sequence of the fundamental is extracted as explained in Section4.3. Root Mean Square(RMS) value of the positive sequence current is summed with output of PI controller. With this,Three synchronized sine functions of the extracted phase of source voltage is multiplied and then subtracted from Load current to form reference current I_{ref}.These reference currents are then compered with the actual output current of DSTATCOM. The difference is then fed to Hysteresis Band PWM, which generates appropriate pulses for the VSI.

4.4.1 Capacitor Voltage Controller

Better operation of DSTATCOM is guaranteed, if the voltage across DC link capacitor is maintained at its reference value. This is achieved by taking inverter losses, P_{loss}, from the source. If capacitor voltage is regulated to a constant reference value, P_{loss} becomes a constant value. To calculate P_{loss}, average dc link voltage (V_{dc}) is compared with a reference voltage (V_{dcref}) and error is passed through a PI controller. Output of the PI controller, P_{loss}, is given as following:

$$P_{loss} = K_p\, e_{vdc} + K_i \int e_{vdc}\, dt \tag{4.20}$$

where $e_{vdc} = (V_{dcref} - V_{dc})$ is voltage error. The terms K_p and K_i are proportional and integral gains respectively. The proper selection of these gains reduces the voltage ripple across the DC link capacitor.

Now we have to generate switching pulses for VSI such that the inverter current follows the reference current. Hysteresis current controller is used for generating this

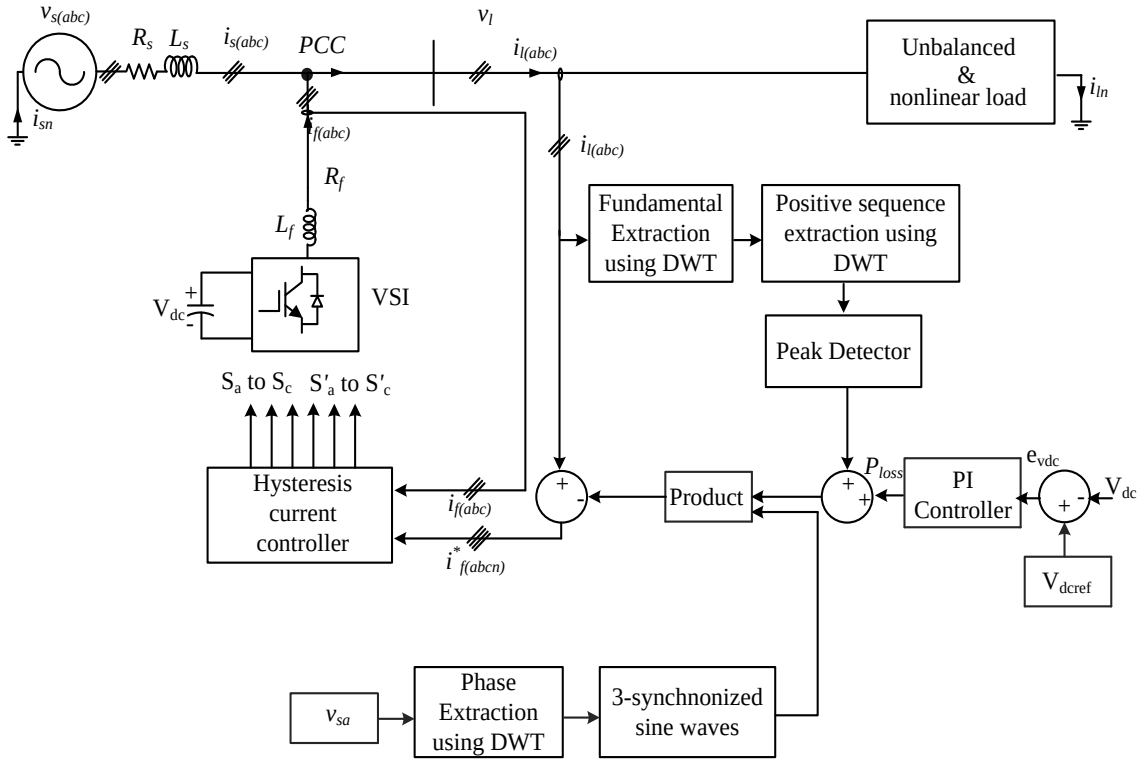

Figure 4.4: DWT based control strategy for DSTATCOM.

pulses for VSI during normal voltage, sag and swell.

4.4.2 Hysteresis Based PWM Controller

The hysteresis band control is used to generate the switching pulses of the shunt inverter. It is an instantaneous feedback system which detects the current error and produces directly the drive commands for the switches when the error exceeds an assigned band. Hysteresis controller is chosen ahead of various other controllers because of its fast dynamics, robust control and ease of implementation. The operation of hysteresis current controller can be understood by observing Fig. 4.5. An upper band and lower band ($+h$ and $-h$) are defined around the shunt inverter reference current. The error is the difference between reference current and actual current. Consider the a phase leg of the three-leg shunt inverter, it has an upper switch S_a and lower switch $S_a^{'}$. Whenever the error goes above $+h$ the upper switch S_a should be turned ON and $S_a^{'}$ should turned OFF. Whenever the error goes below $-h$, complement to the previous operation should take place.

If $error \geq h$ then $u = 1$

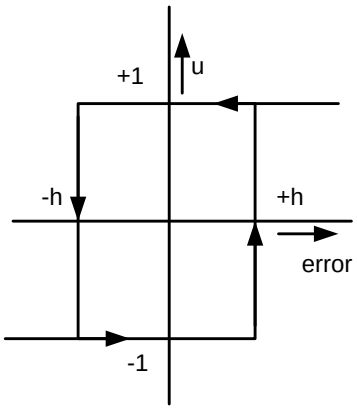

Figure 4.5: Two-level hysteresis scheme.

If $error \leq h$ then $u = -1$

$$\left.\begin{array}{ll} S_a & ON \\ S_a^{'} & OFF \end{array}\right\} \quad u = 1$$

$$\left.\begin{array}{ll} S_a & OFF \\ S_a^{'} & ON \end{array}\right\} \quad u = -1$$

When $u = 1$ the actual current injected by shunt APF increases and when $u = -1$ the current injected by shunt APF decrease.

4.5 Summary

In this chapter, Biorthogonal spline based DWT is proposed for extraction of fundamental component and compensation of the estimated disturbances using DSTATCOM. From the simulation studies, it is found that the proposed method can extract fundamental with less THD. In addition B-spline DWT based phase extraction method has been proposed in this chapter. It is compared with the complex Morlet CWT which showed the accuracy of the proposed method. The proposed method is used as a control algorithm in DSTATCOM. Since the proposed method used DWT, real time implementation is possible with less computational effort.

CHAPTER 5

SIMULATION STUDY

An online discrete wavelet control strategy for DSTATCOM operation is proposed in this project. The proposed control strategy for the DSTATCOM control system is simulated using MATLAB/SIMULINK software. A nonlinear load, which produces unsymmetrical harmonic components and an unsymmetrical load with different impedance in three phases are connected to the load bus to produce fundamental unsymmetrical components in three-phase source voltages. Parameter values of the system shown in Fig. 2.1 are given in Table 5.1. For the sake of simplicity, Fig. 2.1 is reproduced in 5.1. Values given in Table 5.1 are used for the simulation study.

Table 5.1: Parameter values for simulation study

Parameter	Value
DSTATCOM DC link voltage (V_{dc})	700 V
Capacitance (C_{dc})	2200 μF
Utility grid voltage ($V_{s(L-L)}$)	400 V
Fundamental frequency	50 Hz
Feeder resistance, inductance	0.0287 Ω, 0.205 mH
Filter inductance L_f	10 mH,
K_p, K_i for DC link PI controller	0.3, 10
Hysteresis band ($\pm h$)	0.02 A
Unbalanced nonlinear load	Z_a= 30+j 188 Ω Z_b= 40+j 172 Ω Z_c= 50+j 157 Ω 3-ϕ full bridge diode rectifier supplying an R-L (50 Ω - 0.2 H) load

5.1 Normal Operation

The source terminal voltages and load currents are shown in Fig. 5.4(a) and 5.4(c) respectively. To maintain unity power factor fundamental current at the source terminal, DSTATCOM injects currents to the PCC which is shown in Fig. 5.4(d). DSTATCOM

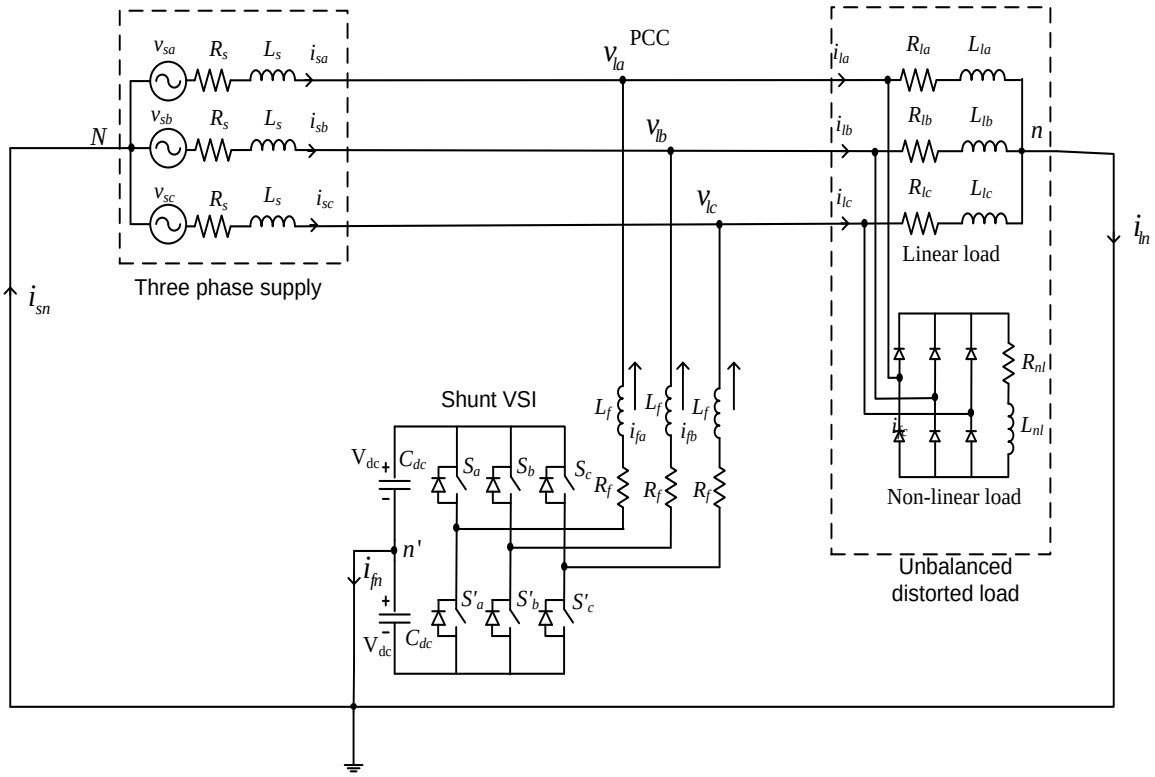

Figure 5.1: Power circuit diagram of DSTATCOM.

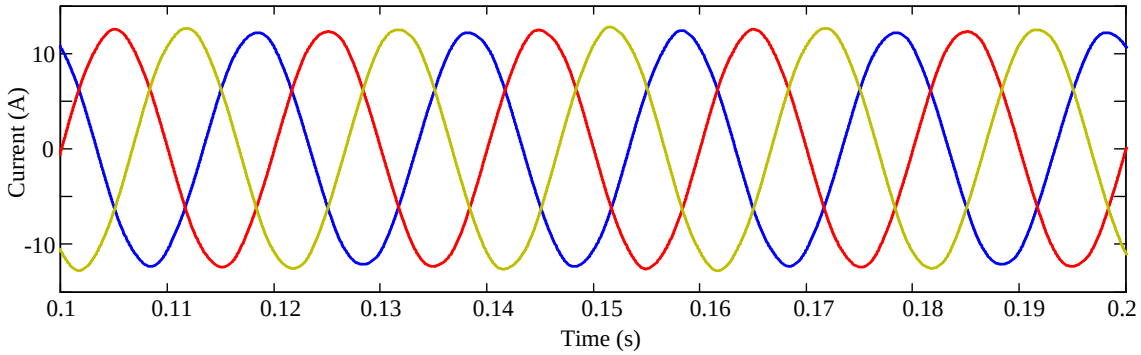

Figure 5.2: Estimated fundamental component of load current using Biorthogonal DWT.

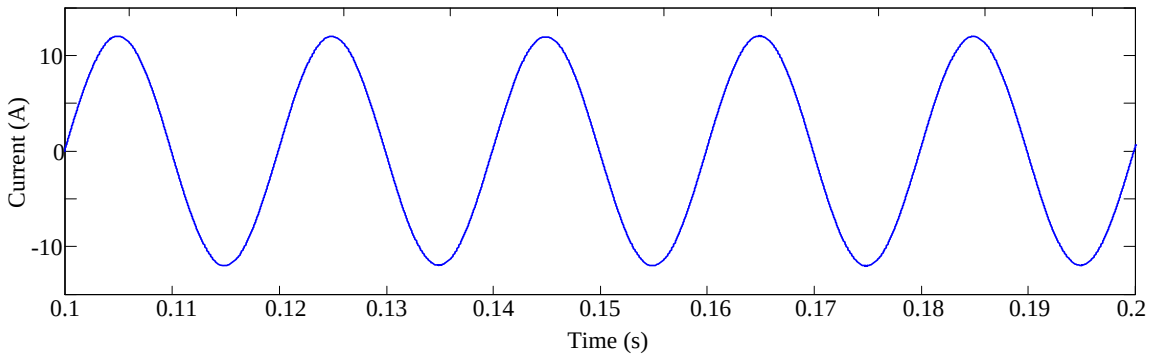

Figure 5.3: Estimated positive sequence of extracted fundamental load current using Biorthogonal DWT.

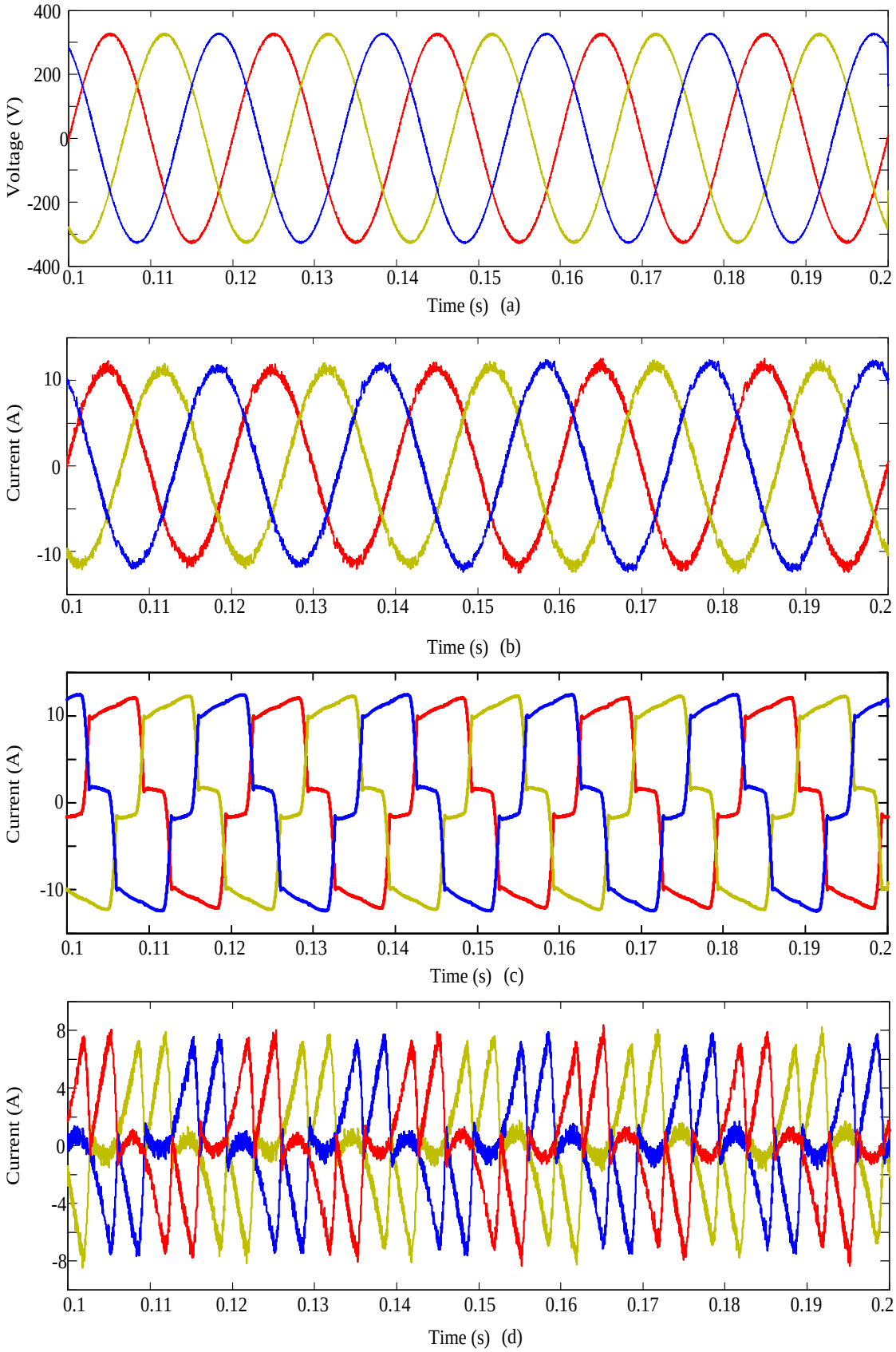

Figure 5.4: (a) Source terminal voltages (b) Source currents (c) Load currents (d) DSTATCOM injected currents.

delivers the load reactive power to maintain unity power factor at the PCC. The DSTATCOM injected currents eliminates the unbalance and harmonics from source currents. The source currents are shown in Fig. 5.4(b). After compensation, THD of source currents has reduced from 24.25% to 3.83%. The fundamental of load current has been extracted using Biorthogonal DWT with THD of 0.88% and is shown in Fig. 5.2. In order to compensate the load unbalance, positive sequence of the unbalanced fundamental of load current has been extracted using Biorthogonal DWT as discussed in Section 4.3. Estimated positive sequence of the fundamental is shown in Fig. 5.3. If there is any phase shift in the source voltage due to voltage sag or any other faults, DSTATCOM still supplies the reactive power demand to the load using the proposed algorithm. It makes use of extracted phase information using biorthogonal DWT discussed in Section 4.2. Phase shift of 30° is applied at $t = 0.2s$ and the resulting source voltage, source current and the phase angle of a-phase voltage are given in Fig. 5.5

5.2 Operation During Voltage Sag

The simulation was done for a 40% voltage sag. The change in source phase rms voltage (p.u) is shown in Fig. 5.6. It occurs at $0.2s$ and the duration of sag is 4 cycles as shown if Fig. 5.7(a). The compensated source currents are given in Fig. 5.7(b). It can be observed from Fig. 5.7(b) that the source currents settle down to the steady state value without many oscillations. In Fig. 5.7(c), it can be seen that load currents have reduced during the voltage sag interval. DSTATCOM injects currents into the PCC as shown in Fig. 5.7(d) which compensates for load harmonics, unbalance and reactive power. The DC link voltage is shown in Fig. 5.7(e) which is maintained at the reference voltage.

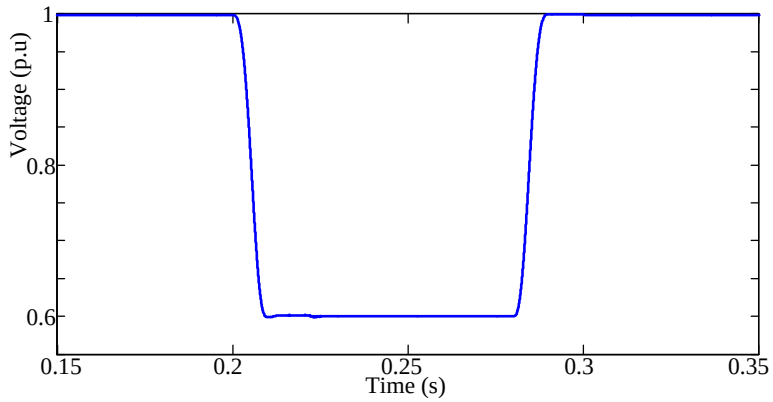

Figure 5.6: Source voltage magnitude variation

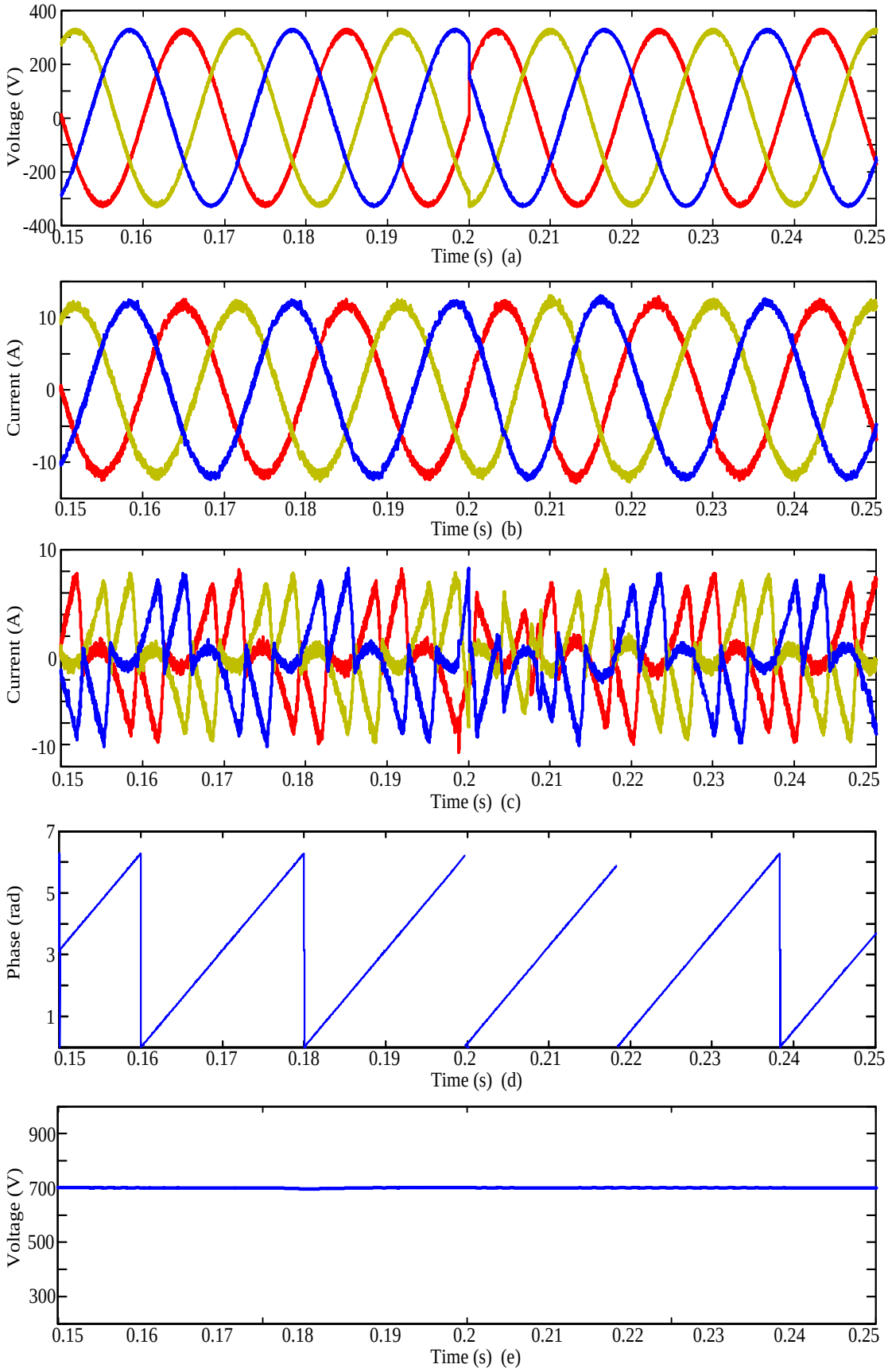

Figure 5.5: Simulation results during phase shift in source voltage at $t = 0.2s$ (a) Source voltages (b) Source currents (c) Injected currents by DSTATCOM (d) Extracted phase information of a phase voltage using Biorthogonal DWT (e) DC link voltage.

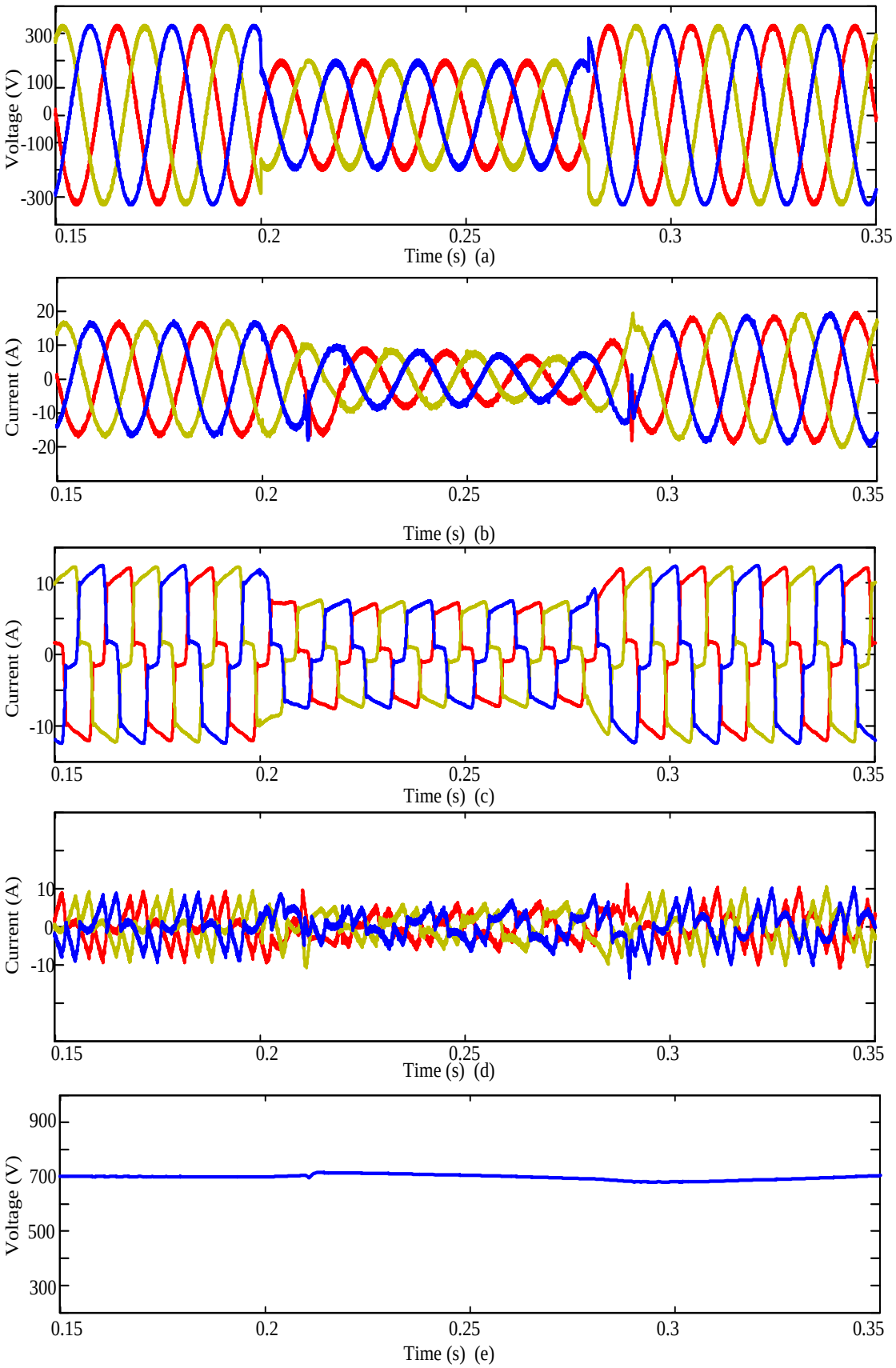

Figure 5.7: Simulation results during voltage sag at $t = 0.2s$ to $t = 0.28s$ (a) Source voltages (b) Source currents (c) Load currents (d) Injected currents by the DSTATCOM (e) DC link voltage.

5.3 Operation During Unbalanced Voltage Sag

A three-phase unbalanced voltage sag is a short-duration reduction in rms voltage in at least one of the three phase or line voltages Unbalanced sag in the power system is associated with line-to-line and single-line-to-ground faults. Non symmetrical faults lead to drops in one, two, or three phases, with not all phases having the same drop. When a voltage sag of 30% is applied on phase a, at $t = 0.3s$ for 5 cycles, magnitude of source currents and load currents have reduced as shown in Fig. 5.8(b) and (c) respectively. It can be observed that the load currents in phase a and b have reduced from their earlier value while load currents in phase c is almost constant. Injected currents by the DSTATCOM is shown in Fig. 5.8(d). From Fig. 5.8(e), it can be observed that the DC link voltage stays at its reference value under the disturbance. It takes less than half cycle for the detection of voltage sag.

5.4 Operation During Voltage Sag with Phase Jump

Voltage sag often defined by two parameters, magnitude and duration. When we characterize a voltage sag through one magnitude and one value for the duration, there are obvious limitations to this method as one e.g. neglects the phase-angle jump. In power systems voltage sag due to a short circuit often changes the phase-angle of the voltage besides its magnitude. Phase jump during a fault is due to the change of the X/R ratio. Most power system equipments are insensitive to phase angle jumps; except power electronic converters using the phase control or zero-crossing switching Simulation studies have been carried out for voltage sag with phase jump and the results are given in Fig. 5.9. When a 40% sag with 20° phase jump is applied as shown in Fig. 5.9(a), source currents are compensated as given in Fig. 5.9(b). It can be observed from Fig. 5.9(c) that the magnitude and phase of load currents have changed accordingly when the sag with phase jump is applied. Fig. 5.9(d) shows the injected currents by DSTATCOM. It can be seen from Fig. 5.9(e) that the DC link voltage remains at the reference value.

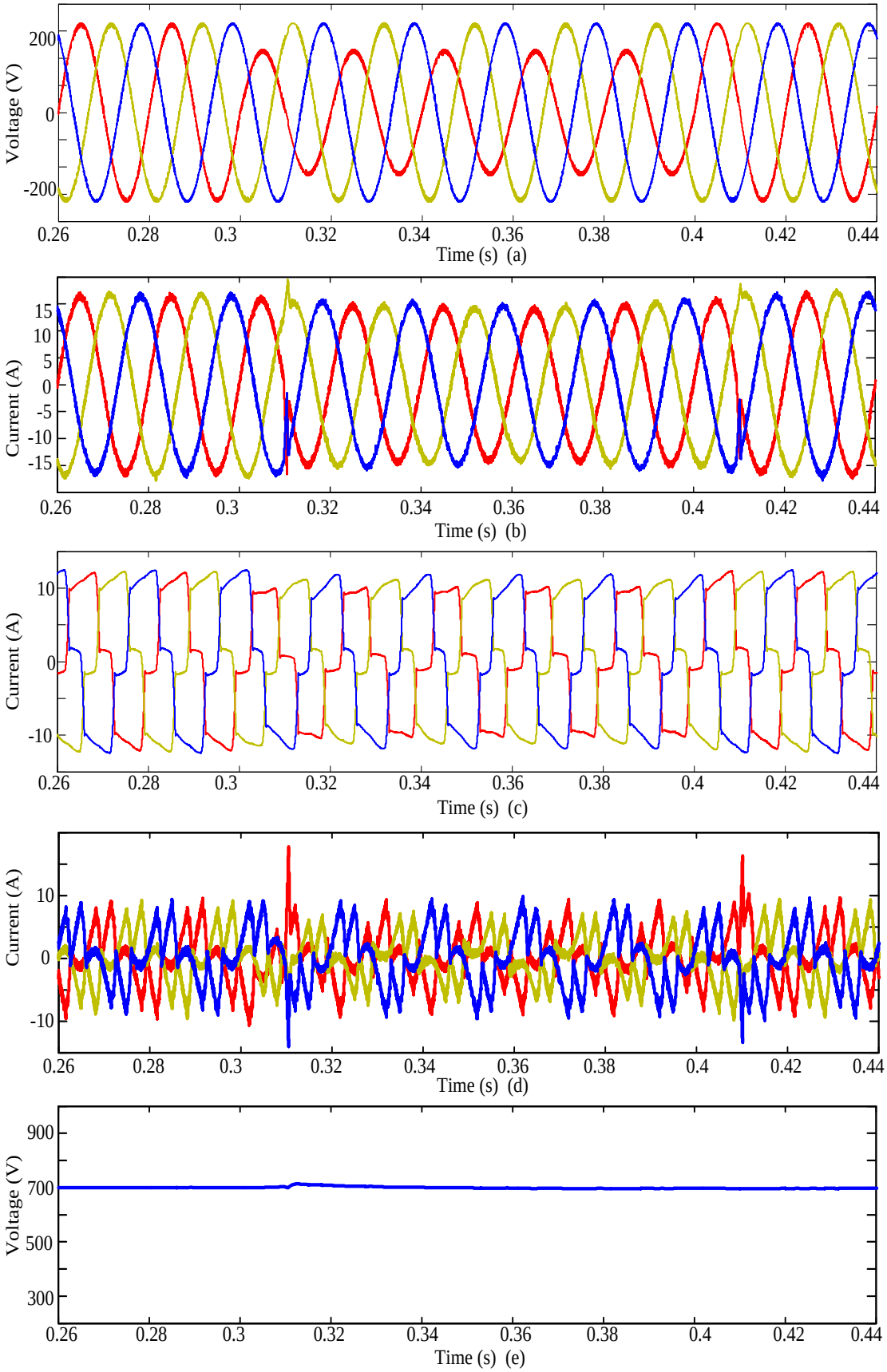

Figure 5.8: Simulation results during unbalanced voltage sag on phase a at t = $0.3s$ upto t = $0.4s$ (a) Source voltages (b) Source currents (c) Load currents (d) Injected currents by DSTATCOM (e) DC link voltage.

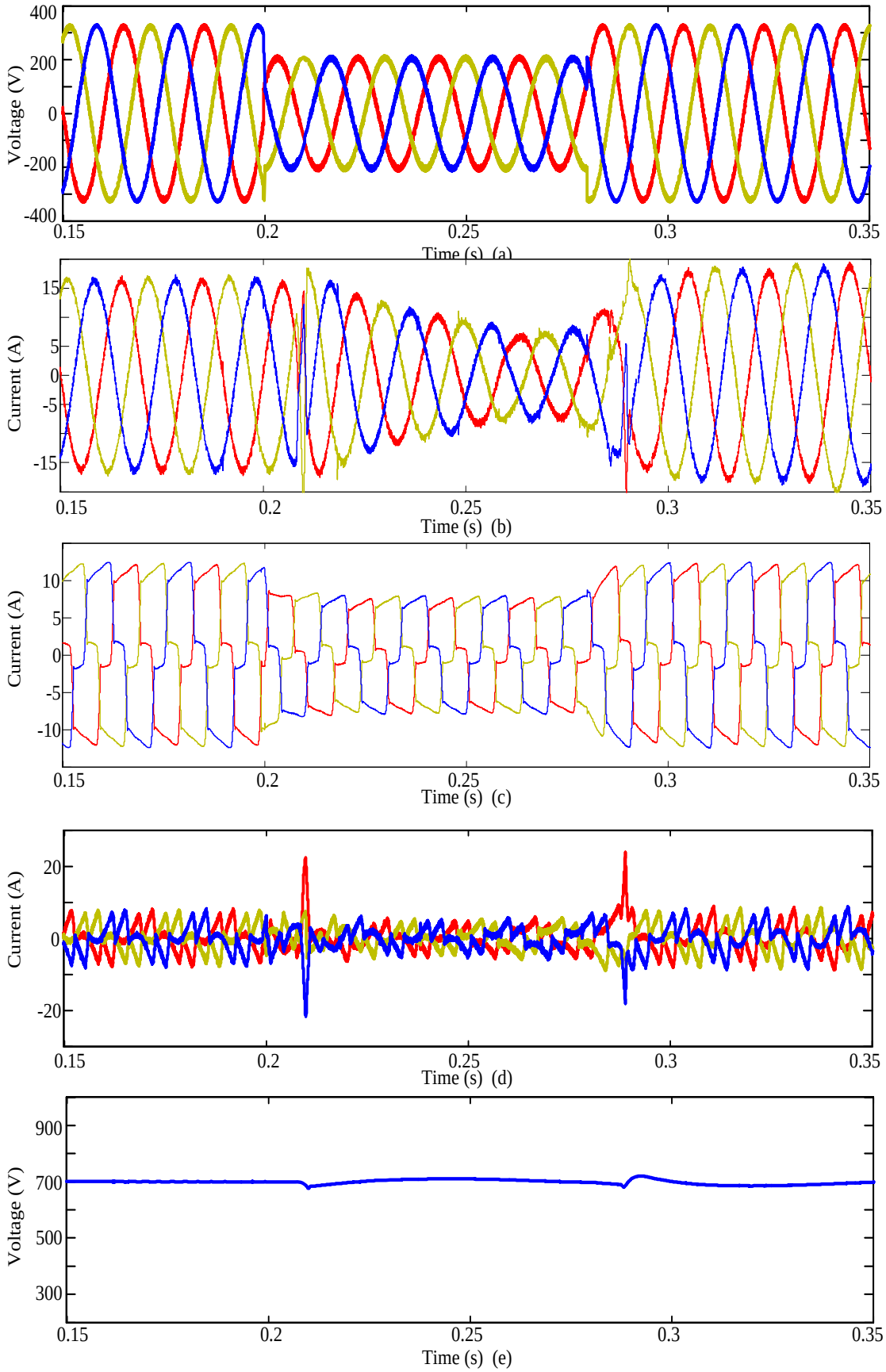

Figure 5.9: Simulation results during voltage sag with phase jump of 20° at $t = 0.2s$ upto $t = 0.28s$ (a) Source voltages (b) Source currents (c) Load currents (d) Injected currents by DSTATCOM (e) DC link voltage.

5.5 Operation Under Load Change

A new 3-phase nonlinear unbalanced load is added in parallel with the existing load at $t = 0.2s$. Details of the newly added load is given in Table 5.2. Load voltages and load currents are given in Fig. 5.10(a) and Fig. 5.10(c) respectively. Since the load currents increase during load change, injected currents by the DSTATCOM also increases accordingly as shown in Fig. 5.10(d). From Fig. 5.10(e), it can be inferred that the DC link voltage remains constant during the load change.

Table 5.2: Newly added load in parallel to the existing load

Unbalanced linear load	Z_a= 125+j 47 Ω Z_b= 130+j 31 Ω Z_c= 150+j 31 Ω
Nonlinear load	3-ϕ full bridge diode rectifier supplying an R-L (250 Ω - 0.15 H) load

5.6 Operation During Variation in Frequency

Unlike the FFT algorithm, the DWT does not extract the amplitude and phase angle of a special frequency component of a distorted signal. For example, if the fundamental frequency of a distorted waveform is 50 Hz, DWT can extract the frequency components between 40 Hz and 60 Hz as fundamental component of the distorted waveform. Thus, if the fundamental frequency deviates from its nominal value (50 Hz), the DWT can still extract the fundamental component of the distorted waveform. Moreover, the proposed method can extract the fundamental frequency rapidly. These benefits render the wavelet-based technique to be less sensitive to frequency oscillation.

Simulation is done for a source voltage frequency variation of 2.5 Hz at $t = 0.2s$ as shown in Fig. 5.11(a) and the compensated source currents are given in Fig. 5.11(b). Load currents and the extracted fundamental component of phase a load current using biorthogonal DWT under frequency variation are given in Fig. 5.11(c) and Fig. 5.11(d). Fig.5.11(e) shows the DC link voltage which remains at the reference value under the frequency variation.

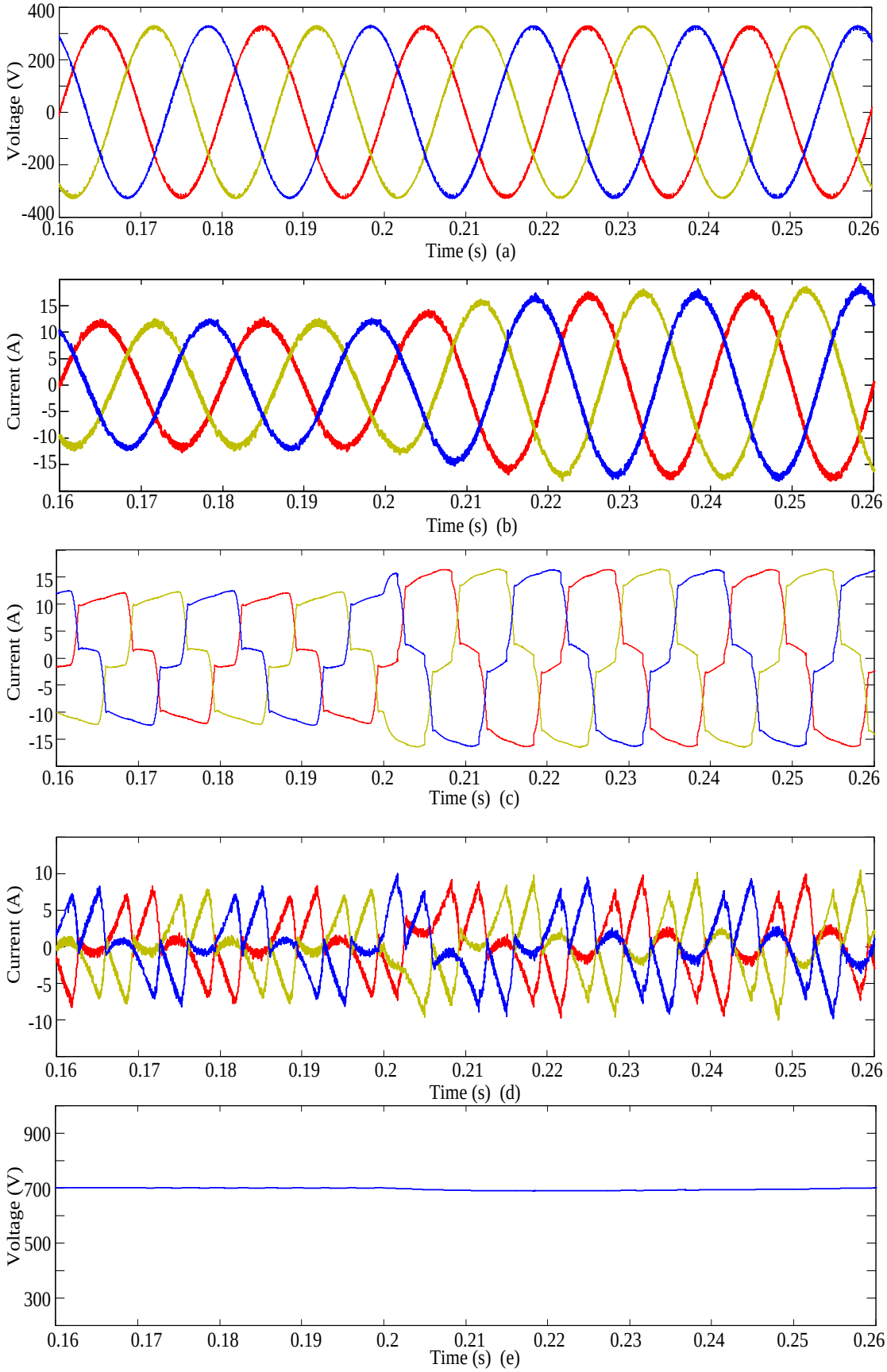

Figure 5.10: Simulation results during load change at $t = 0.2s$ (a) Load voltages (b) Source currents (c) Load currents (d) Injected currents by DSTATCOM (e) DC link voltage.

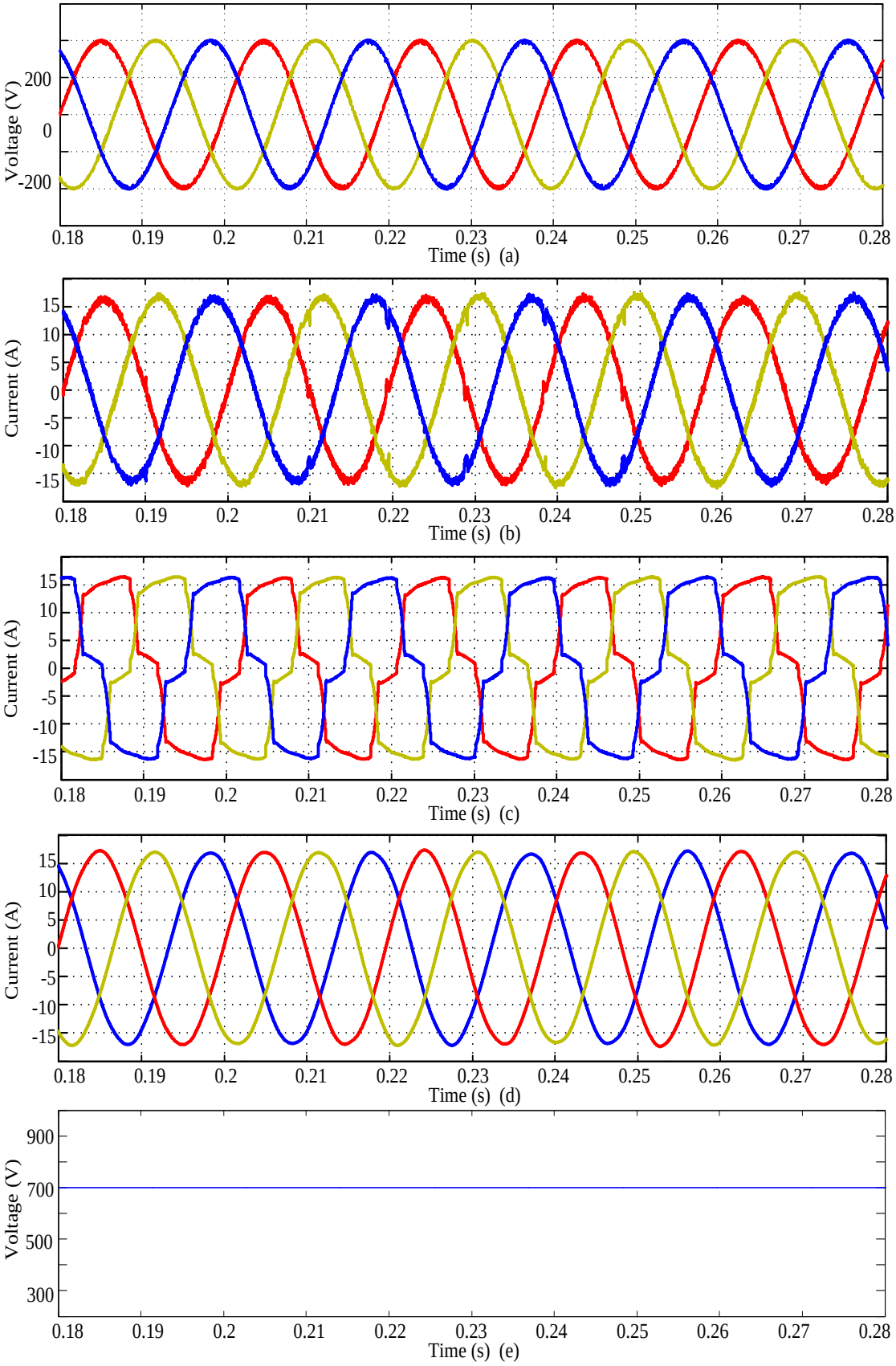

Figure 5.11: Simulation results during frequency change at $t = 0.2s$ (a) Source voltages (b) Source currents (c) Load currents (d) Extracted fundamental component of load current (e) DC link voltage.

CHAPTER 6

CONCLUSION AND SCOPE FOR FUTURE WORK

6.1 Summary

Power quality has raised as a topical issue in power systems in the 1990s which largely coincides with the huge advancements achieved in the computing technology and information theory. This advancement in signal processing has to be utilized in order to mitigate the power quality disturbances. Signal processing is generally used when there is a need to extract specific information from the raw data, which typically in power systems are the voltage and current waveforms. Any disturbance in these quantities has to be identified, classified and characterized followed by solution assessment and design. Fourier theory has been the core of many traditional techniques to address these issues and it is still widely used today. However, it is increasingly being replaced by newer approaches notably wavelet transform and especially in the post-event processing of the time-varying phenomena.

In this thesis, detection and characterization of power quality disturbances using wavelet transform based technique has been discussed. Performance of the proposed method to detect and characterize voltage sag and capacitor switching transient is evaluated through simulation studies. In addition, this project mainly focuses on wavelet based reference quantity generation technique for a custom power device, DSTACOM. Distribution system with nonlinear unbalanced load compensated by DSTATCOM is modeled in Matlab/Simulink for simulation studies.Limitations of time based control algorithms such as instantaneous symmetrical component theory and pq theory are discussed in detail in this thesis. Advantages of Wavelet based control algorithm over other frequency based methods such as Fourier analysis and Short Term Fourier Transform (STFT) are also presented. Hence Wavelet transform based signal processing is proposed for fast and accurate estimation of reference signals of DSTATCOM. The conventional CWT is considered to have high computational burden and redundant. Even though DWT requires less computation burden and non redundant, it is thought to have

lack of phase information which makes it unfit for reference quantity generation. But in this project, a new method to extract phase information using DWT has been proposed. DWT has been proven to have the ability to extract fundamental and positive sequence accurately and rapidly which makes it suitable for reference quantity generation. Biorthogonal 5.5 wavelet is chosen as the mother wavelet for DWT. Advantages of Biorthogonal DWT over other wavelet based techniques can be summerized as given below.

- Biorthogonal RDWT is as accurate as Meyer DWT and conventional CWT with less computational burden.
- Compared to conventional CWT, computational cost of Biorthogonal DWT is N times less (where N is the length of the analysed signal).
- Since Biorthonal DWTs are loss-less ones which means that all information of the analyzed signal is conserved in wavelet coefficients of the DWTs, phase information can be extracted by proper approach.
- It is easy to implement the DWT algorithm in real time using a digital signal processor, since all the signals used for the analysis are discrete signals.

Detailed simulation studies are carried out for various cases such as estimation of fundamental current, source current compensation under voltage sag with phase angle jump, unbalanced voltage sag, load change and system frequency variation. The proposed Biorthogonal DWT based algorithm is found to have produce accurate results under these disturbances. Significant contributions as a result of this work can be outlines as the following.

- Fast and accurate detection and characterization of the power quality disturbances are possible by using DWT
- The proposed biorthogonal DWT can be used to extract the phase information of signals, with accuracy and less computational cost.
- DSTACOM along with the proposed Biorthogonal DWT based reference signal estimator can be utilized as the compensating device for both source and load related power quality problems.
- The proposed Biorthogonal DWT can be used for fast and accurate compensation of source current under voltage sag with phase jump, unbalanced voltage sag, load change and frequency variation.
- Frequency variation in the power system does not affect the performance of fundamental extraction and other reference quantity estimation.

6.2 Scope for Future Work

Following are the future scopes of the work done in this thesis.

- The proposed DWT based reference quantity generation can be used to mitigate the voltage related power quality issues in the distribution system since the wavelet based technique for fundamental positive sequence extraction of load current used in this project can be applied for voltage signal as well. Hence the proposed reference generation technique can be used in other custom power devices such as UPQC.
- The proposed Biorthogonal DWT which has been validated by simulation studies could be implemented in DSP/FPGA to enable it to be used for real-time applications.

As the understanding of wavelet transform grows, there will be more attempts at applying it to power quality analysis in order to improve the performance of the custom power devices.

REFERENCES

[1] D. Flinn, C. Gilker, and S. Mendis, "Methods for identifying potential power quality problems," in *Rural Electric Power Conference, 1991. Papers Presented at the 35th Annual Conference*, Apr 1991, pp. C1/1–C1/5.

[2] J. Arrillaga, M. Bollen, and N. Watson, "Power quality following deregulation," *Proceedings of the IEEE*, vol. 88, no. 2, pp. 246–261, Feb 2000.

[3] A. Kapoor and R. Mahanty, "A quasi passive filter for power quality improvement," in *Industrial Technology 2000. Proceedings of IEEE International Conference on*, vol. 1, Jan 2000, pp. 526–529 vol.2.

[4] D. Sutanto, M. Bou-rabee, K. Tam, and C. Chang, "Harmonic filters for industrial power systems," in *Advances in Power System Control, Operation and Management, 1991. APSCOM-91., 1991 International Conference on*, Nov 1991, pp. 594–598 vol.2.

[5] P. Salmeron and S. Litran, "Improvement of the electric power quality using series active and shunt passive filters," *Power Delivery, IEEE Transactions on*, vol. 25, no. 2, pp. 1058–1067, April 2010.

[6] B. Singh, K. Al-Haddad, and A. Chandra, "A review of active filters for power quality improvement," *Industrial Electronics, IEEE Transactions on*, vol. 46, no. 5, pp. 960–971, Oct 1999.

[7] J. Hafner, M. Aredes, and K. Heumann, "A shunt active power filter applied to high voltage distribution lines," *Power Engineering Review, IEEE*, vol. 17, no. 1, pp. 51–52, January 1997.

[8] N. Woodley, L. Morgan, and A. Sundaram, "Experience with an inverter-based dynamic voltage restorer," *Power Delivery, IEEE Transactions on*, vol. 14, no. 3, pp. 1181–1186, Jul 1999.

[9] H. Fujita and H. Akagi, "A practical approach to harmonic compensation in power systems-series connection of passive and active filters," in *Industry Applications Society Annual Meeting, 1990., Conference Record of the 1990 IEEE*, Oct 1990, pp. 1107–1112 vol.2.

[10] P.-T. Cheng, S. Bhattacharya, and D. Divan, "Hybrid solutions for improving passive filter performance in high power applications," in *Applied Power Electronics Conference and Exposition, 1996. APEC '96. Conference Proceedings 1996., Eleventh Annual*, vol. 2, Mar 1996, pp. 911–917 vol.2.

[11] P. T. Cheng, S. Bhattacharya, and D. Divan, "Control of square-wave inverters in high-power hybrid active filter systems," *Industry Applications, IEEE Transactions on*, vol. 34, no. 3, pp. 458–472, May 1998.

[12] A. Bhattacharya, C. Chakraborty, and S. Bhattacharya, "Parallel-connected shunt hybrid active power filters operating at different switching frequencies for improved performance," *Industrial Electronics, IEEE Transactions on*, vol. 59, no. 11, pp. 4007–4019, Nov 2012.

[13] "Ieee recommended practice for monitoring electric power quality," *IEEE Std 1159-2009 (Revision of IEEE Std 1159-1995)*, pp. c1–81, June 2009.

[14] S. Jain, P. Agrawal, and H. Gupta, "Fuzzy logic controlled shunt active power filter for power quality improvement," *Electric Power Applications, IEE Proceedings -*, vol. 149, no. 5, pp. 317–328, Sep 2002.

[15] G.-H. Choe and M.-H. Park, "Analysis and control of active power filter with optimized injection," *Power Electronics, IEEE Transactions on*, vol. 4, no. 4, pp. 427–433, Oct 1989.

[16] H. Akagi, Y. Kanazawa, and A. Nabae, "Instantaneous reactive power compensators comprising switching devices without energy storage components," *Industry Applications, IEEE Transactions on*, vol. IA-20, no. 3, pp. 625–630, May 1984.

[17] F. Z. Peng and J.-S. Lai, "Generalized instantaneous reactive power theory for three-phase power systems," *Instrumentation and Measurement, IEEE Transactions on*, vol. 45, no. 1, pp. 293–297, Feb 1996.

[18] F. Peng, G. Ott Jr, and D. Adams, "Harmonic and reactive power compensation based on the generalized instantaneous reactive power theory for three-phase four-wire systems," *IEEE Transactions on Power Electronics*, vol. 13, no. 6, pp. 1174–1181, 1998.

[19] A. Ghosh and A. Joshi, "The use of instantaneous symmetrical components for balancing a delta connected load and power factor correction," *Electric Power Systems Research*, vol. 54, no. 1, pp. 67–74, 2000.

[20] U. Rao, Mahesh. K. Mishra, and A. Ghosh, "Control strategies for load compensation using instantaneous symmetrical component theory under different supply voltages," *IEEE Transactions on Power Delivery*, vol. 23, no. 4, pp. 2310–2317, 2008.

[21] A. Ghosh and A. Joshi, "A new method for load balancing and power factor correction using instantaneous symmetrical components," *IEEE Power Engineering Review*, vol. 18, no. 9, pp. 60–61, 1998.

[22] A. Chaoui, J.-P. Gaubert, F. Krim, and L. Rambault, "On the design of shunt active filter for improving power quality," in *Industrial Electronics, 2008. ISIE 2008. IEEE International Symposium on*, June 2008, pp. 31–37.

[23] M. Benhabib and S. Saadate, "New control approach for four-wire active power filter based on the use of synchronous reference frame," *Electric Power Systems Research*, vol. 73, no. 3, pp. 353 – 362, 2005.

[24] C. Chen, C. Lin, and C. Huang, "Reactive and harmonic current compensation for unbalanced three-phase systems using the synchronous detection method," *Electric power systems research*, vol. 26, no. 3, pp. 163–170, 1993.

[25] A. Bruce, D. Donoho, and H.-Y. Gao, "Wavelet analysis [for signal processing]," *Spectrum, IEEE*, vol. 33, no. 10, pp. 26–35, Oct 1996.

[26] A. Graps, "An introduction to wavelets," *Computational Science Engineering, IEEE*, vol. 2, no. 2, pp. 50–61, Summer 1995.

[27] S. Mallat, *A wavelet tour of signal processing*. Academic press, 1999.

[28] S. Kang, H. Zhang, and Y. Kang, "Simulation analysis of time-frequency based on waveform detection technique for power quality application," in *Control and Decision Conference (CCDC), 2010 Chinese*, May 2010, pp. 2529–2532.

[29] C.-H. Lin and M.-C. Tsao, "Power quality detection with classification enhancible wavelet-probabilistic network in a power system," *Generation, Transmission and Distribution, IEE Proceedings-*, vol. 152, no. 6, pp. 969–976, Nov 2005.

[30] S. Chen and H. Y. Zhu, "Wavelet transform for processing power quality disturbances," *EURASIP Journal on Applied Signal Processing*, vol. 2007, no. 1, pp. 176–176, 2007.

[31] C. H. Kim and R. Aggarwal, "Wavelet transforms in power systems. i. general introduction to the wavelet transforms," *Power Engineering Journal*, vol. 14, no. 2, pp. 81–87, April 2000.

[32] ——, "Wavelet transforms in power systems. part 2: Examples of application to actual power system transients," *Power Engineering Journal*, vol. 15, no. 4, pp. 193–202, 2001.

[33] S. Kamble, S. Mate, and M. Waware, "Online wavelet based control algorithm for shunt active power filter operation," in *Control Applications (CCA), 2013 IEEE International Conference on*, Aug 2013, pp. 1153–1158.

[34] D. C. Robertson, O. I. Camps, J. S. Mayer, and W. B. Gish, "Wavelets and electromagnetic power system transients," *Power Delivery, IEEE Transactions on*, vol. 11, no. 2, pp. 1050–1058, 1996.

[35] O. Poisson, P. Rioual, and M. Meunier, "Detection and measurement of power quality disturbances using wavelet transform," *Power Delivery, IEEE Transactions on*, vol. 15, no. 3, pp. 1039–1044, Jul 2000.

[36] S. Santoso, W. Grady, E. Powers, J. Lamoree, and S. Bhatt, "Characterization of distribution power quality events with fourier and wavelet transforms," *Power Delivery, IEEE Transactions on*, vol. 15, no. 1, pp. 247–254, Jan 2000.

[37] N. Karthikeyan, Mahesh. K. Mishra, and B. Kumar, "Complex wavelet based control strategy for upqc," in *Power Electronics, Drives and Energy Systems (PEDES) 2010 Power India, 2010 Joint International Conference on*, Dec 2010, pp. 1–6.

[38] M. Unser and A. Aldroubi, "A review of wavelets in biomedical applications," *Proceedings of the IEEE*, vol. 84, no. 4, pp. 626–638, Apr 1996.

[39] W. Wilkinson and M. Cox, "Discrete wavelet analysis of power system transients," *Power Systems, IEEE Transactions on*, vol. 11, no. 4, pp. 2038–2044, Nov 1996.

[40] X. Chen, "Real wavelet transform-based phase information extraction method: Theory and demonstrations," *Industrial Electronics, IEEE Transactions on*, vol. 56, no. 3, pp. 891–899, March 2009.

[41] C. Xiangxun, "Wavelet-based method for tracking flicker level," in *Precision Electromagnetic Measurements Digest, 2004 Conference on*, June 2004, pp. 364–365.

[42] W. Morsi and M. El-Hawary, "Reformulating three-phase power components definitions contained in the ieee standard 1459 ndash;2000 using discrete wavelet transform," *Power Delivery, IEEE Transactions on*, vol. 22, no. 3, pp. 1917–1925, July 2007.